

Fabrication and Characterization of “Nano-Beakers” for the Synthesis of Ceramic  
Colloids

by

Hannah M. Zukswert

A thesis presented to the faculty of Mount Holyoke College  
in partial fulfillment of the requirements for the degree of  
Bachelor of Arts with Honors

Department of Chemistry  
South Hadley, Massachusetts

May 2011

This thesis was prepared under  
the direction of Dr. Greg Roman  
for eight credits

## Acknowledgements

First and foremost, I would like to thank Greg Roman for seeing this project through to its completion and for giving me the opportunity to do this work in the first place. I have so appreciated your support and guidance in this project as well as in my struggle to figure out what to do with my life after graduation.

Thank you to Marian Rice for training me to use the scanning electron microscope and sputter coater so that I could image the many samples of microspheres that I synthesized.

Thank you to Madelaine Denno for her help in collecting some of the preliminary data in Chapter 1, and to Jessica McKenzie for teaching me how to microfabricate microfluidic devices.

Thank you also to the faculty and staff of the Mount Holyoke Chemistry Department, particularly Darren Hamilton, Maria Gomez, and Dina Bevivino, for their continual support of my studies and for making my time here memorable.

This research was supported in part by the American Chemical Society Petroleum Research Fund

## Table of Contents

Acknowledgements	iii
Table of Contents	iv
List of Figures	vii
List of Tables	ix
Abstract	x
<b>Chapter 1—Microfluidics</b>	<b>1</b>
<b>1.1 Introduction to Microfluidics</b>	<b>1</b>
1.1.1 History of Microfluidics and Separation Science	1
1.1.2 Advantages and Applications of Microfluidic Techniques	4
1.1.3 Flow Regimes and Regime Characterization	7
1.1.4 Single Phase Flows in Microchannels	10
1.1.5 Multiphase Flows in Microchannels	12
<b>1.2 Fabrication and Operation of Microfluidic Devices</b>	<b>24</b>
1.2.1 Microfabricated Devices	24
1.2.2 Microfluidic Devices Constructed with Commercially Available Fluidics	29
1.2.3 Ancillary Components	36
<b>1.3 Experimental Methods—Characterization of Segmented Flow</b>	<b>38</b>
1.3.1 Construction of the Reactors	38
1.3.2 Characterization of the Segmented Flow Microreactor	40
<b>1.4 Results and Discussion</b>	<b>43</b>

<b>Chapter 2—Sol-Gel Synthesis of Ceramic Microspheres</b>	<b>48</b>
<b>2.1 Introduction to Sol-Gel Chemistry</b>	<b>48</b>
2.1.1 Reproducible and Monodisperse Ceramic Microspheres	48
2.1.2 Sol-Gel Chemistry	50
2.1.3 History of Sol-Gel Chemistry	52
2.1.4 The Process	54
2.1.5 Synthesis of Silica Microspheres	55
2.1.6 Synthesis of Titania Microspheres	60
<b>2.2 Experimental Methods—Synthesis of Ceramic Microspheres</b>	<b>63</b>
2.2.1 Materials for the Synthesis of Silica	63
2.2.2 Characterization of Batch Synthesis of Silica	63
2.2.3 Characterization of Single Phase and Segmented Flow Synthesis of Silica	64
2.2.4 Materials for the Synthesis of Titania	68
2.2.5 Characterization of Batch Synthesis of Titania	68
2.2.6 Characterization of Single Phase Flow Synthesis of Titania	69
<b>2.3 Results and Discussion</b>	<b>72</b>
2.3.1 Batch Synthesis of Silica	72
2.3.2 Single Phase Microreactor Synthesis of Silica	76
2.3.3 Segmented Flow Synthesis of Silica	85
2.3.4 Batch Synthesis of Titania	90
2.3.5 Single Phase Microreactor Synthesis of Titania	92

<b>Chapter 3—Conclusions</b>	<b>96</b>
<b>3.1 Characterization of Segmented Flow</b>	<b>96</b>
<b>3.2 Characterization of Ceramic Microsphere Synthesis</b>	<b>97</b>
3.2.1 Batch Reactor	97
3.2.2 Single Phase Microreactor	98
3.2.3 Segmented Flow Microreactor	99
<b>3.3 Comparison with the Literature</b>	<b>101</b>
<b>3.4 Future Work</b>	<b>103</b>
References	104

## LIST OF FIGURES

Figure 1.1	Microfluidic devices	5
Figure 1.2	Mixing by diffusion in laminar flows	7
Figure 1.3	Parabolic velocity flow profile	11
Figure 1.4	Types of segmented flows	13
Figure 1.5	Wall spanning segmented flows	15
Figure 1.6	Optical microscope image of periodic segmented flow	17
Figure 1.7	Formation of oil/water segmented flow	19
Figure 1.8	Velocity vectors of recirculation within a plug	23
Figure 1.9	Chaotic advection induced by patterned channel surfaces	24
Figure 1.10	Photolithography process	26
Figure 1.11	Mechanism of chain scission of PMMA	27
Figure 1.12	Soft-lithography process	29
Figure 1.13	Single phase microreactor used in this project	30
Figure 1.14	Segmented flow microreactor used in this project	31
Figure 1.15	Microfluidic T-junction	32
Figure 1.16	A steel and PEEK union	33
Figure 1.17	Machine schematic for fused-silica capillary production	35
Figure 1.18	Single phase microreactor with reagent flow path	39
Figure 1.19	Segmented flow microreactor with reagent flow path	40
Figure 1.20	Igor Pro image line profile	42
Figure 1.21	Wall spanning plugs in the segmented flow microreactor	43
Figure 1.22	Average volume of aqueous plugs under different phase flow rates	44
Figure 1.23	Average rate of aqueous plug flow under different phase flow rates	46
Figure 2.1	SEM image of silica microspheres produced in a batch reactor	49
Figure 2.2	The sol-gel process	51
Figure 2.3	Tetraethoxysilane (TEOS) precursor for silica synthesis	56
Figure 2.4	Mechanism for base catalyzed hydrolysis of a silicon alkoxide	56
Figure 2.5	Mechanism for acid catalyzed hydrolysis of a silicon alkoxide	57
Figure 2.6	Average diameter of silica microspheres produced by batch synthesis as determined from SEM images	73
Figure 2.7	Average diameter of silica microspheres produced in the single phase microreactor with an aging capillary with an ID of 150 $\mu\text{m}$ . This data was gathered from SEM images	77

Figure 2.8	Average diameter of silica microspheres produced in the single phase microreactor with an aging capillary with an ID of 150 $\mu\text{m}$ . This data was gathered from DLS measurements	78
Figure 2.9	Average diameter of silica microspheres produced in the single phase microreactor with an aging capillary with an ID of 250 $\mu\text{m}$ . This data was collected from SEM images	81
Figure 2.10	Average diameter of silica microspheres produced in the single phase microreactor with an aging capillary with an ID of 250 $\mu\text{m}$ . This data was gathered from DLS results	82
Figure 2.11	Average diameter of silica microspheres produced in the segmented flow microreactor. This data was collected from SEM images	85
Figure 2.12	Average diameter of silica microspheres produced in the segmented flow microreactor. This data was collected from DLS measurements	86
Figure 2.13	Average diameter of titania microspheres produced in the single phase microreactor. This data was collected from SEM images	93



LIST OF TABLES

Table 2.1	Microreactor settings for silica synthesis in the single phase microreactor	65
Table 2.2	Flow rates of reagents and gas in the segmented flow microreactor	68
Table 2.3	Microreactor settings for titania synthesis in the single phase microreactor	70
Table 2.4	SEM images of silica microspheres produced in the batch reactor	75
Table 2.5	Results for 20 minute residence time samples from different batches of silica	76
Table 2.6	SEM images of silica microspheres produced in the single phase microreactor with an aging capillary with an ID of 150 $\mu\text{m}$	80
Table 2.7	SEM images of silica microspheres produced in the single phase microreactor with an aging capillary with an ID of 250 $\mu\text{m}$	84
Table 2.8	SEM images of silica microspheres produced in the segmented flow microreactor	87
Table 2.9	Microsphere diameters for the batch synthesis of titania	90
Table 2.10	SEM images of titania produced by preliminary batch syntheses for different reagent concentrations	91
Table 2.11	SEM images of titania produced in the single phase microreactor	94

## ABSTRACT

Microreactors are devices containing microscale channel networks, called microfluidics, in which a variety of reactions and analysis schemes can be performed. They allow for precisely controlled reaction times and mixing rates, higher yields, smaller waste production, reproducible multi-phase flow patterns, and an ability to scale-up the method to produce larger volumes of product.<sup>3</sup>

Ceramic microspheres, such as those made of silica or titania, show promise for improving current methods and materials of many applications, ranging from medical imaging and drug delivery, renewable energy, and chromatography, to name a few. The microspheres can be easily synthesized by sol-gel chemistry using batch methods, however, the products are often polydisperse and their sizes irreproducible.<sup>3</sup> Segmented flow microreactors offer a solution to these problems with their highly controllable reaction times, enhanced mixing capabilities, and reproducible reaction conditions that are made possible by isolating the reaction in a series of periodically spaced “nano-beakers”.<sup>5</sup>

In this project, silica and titania microspheres were synthesized in three different reactors: a batch reactor (essentially a beaker), a single phase microreactor, and a segmented flow microreactor. It was hypothesized that the microspheres with the narrowest size distribution would be produced by the segmented flow microreactor involving nano-beakers, followed by the batch reactor, and finally the single phase microreactor. The microreactors were not

microfabricated, as is the usual method of device production, but were constructed from commercially available T-junctions, capillaries, and pumps. This project represents the first time that a microreactor built with commercially available capillary fluidics has been used to synthesize microparticles using segmented flows.

First, the segmented flow microreactor was characterized to understand the effect that reagent flow rates have on the volume and periodicity of the nanobeads. Then, the average diameter and size distribution of microspheres produced by each reactor were measured after several different reaction times by dynamic light scattering as well as from images taken on a scanning electron microscope.

Microspheres were successfully produced in the single phase microreactor, demonstrating that capillary-based microreactors are a viable alternative to microfabricated devices. Contrary to expectations, the segmented flow microreactor produced microspheres with the widest size distribution. SEM images suggest that the problem lies in the distribution of reagents into the nanobeads upon segmentation, disrupting the development of microspheres with a defined morphology. Further investigation into how the reagents are distributed and how flow rates and capillary dimensions affect this would help to improve the segmented flow microreactor and achieve better results.

## CHAPTER 1—MICROFLUIDICS

### 1.1 Introduction to Microfluidics

#### *1.1.1 History of Microfluidics and Separation Science*

Microfluidics allow for the manipulation and chemical analysis of fluids at the micro to nanoliter scale. This manipulation is typically achieved in micro- or nano-fabricated channels, or lab-on-a-chip devices, which confine fluids to a multiplexed system of microchannels, enabling multi-step reactions or analyses to be carried out in the space of a few square centimeters (i.e. about the size of a postage stamp).<sup>2,3,7,13</sup> The first silicon micro analysis system was created by Stanford University scientists Terry, Jerman, and Angell in 1979, who developed a gas chromatography air analyzer on a silicon wafer with an area a little larger than 2 in<sup>2</sup>.<sup>2</sup>

An understanding of fluid dynamics preceded the existence of the technology necessary to fabricate and manipulate fluids at such small scales. Stokes and Navier made substantial contributions to fluid dynamic theory early in the nineteenth century and Hagen and Poiseuille carried out capillary experiments later in the century. In the 1950's Taylor made significant contributions to the understanding of fluid dynamics with his studies of diffusion and dispersion under laminar flow conditions.<sup>6</sup>

The development of the technology necessary for the fabrication of microscale devices is rooted in the study of chromatographic separations in which packed particle beds were used to partition molecules of differing polarity and perform chemical separations. The fluids between these packed particles were of microscale volumes, and exhibited many of the physical characteristics typical of modern day microfluidic manifolds.<sup>1</sup>

Advancements in the field of chromatography were made in the middle of the twentieth century by Golay and van Deemter who theorized that separations could be improved by decreasing the diameter of open separation columns, thereby increasing the surface area to volume ratio. By the late 1980's capillaries with an inner diameter of 75  $\mu\text{m}$  were being used. The evolution of capillaries was a natural progression that fed into the development of microfluidic technologies in the late 90's and continues today.<sup>6, 43</sup>

Interest in the development of microscale devices piqued in 1960 when a talk given by physicist Richard Feynman, a professor at the California Institute of Technology, was published in *Engineering and Science* magazine. The piece, titled "There's Plenty of Room at the Bottom", encouraged the miniaturization of devices to be pushed even further, suggesting that an entire encyclopedia be written on the head of a pin.<sup>43, 44, 45</sup> This article was successful in triggering an interest in miniaturizing electronic devices, so much so that the achievable integration density of devices grew according to Moore's law and doubled every

18 months or so until the late 1990's, at which point it had reached the limits of photolithographic capabilities.<sup>43</sup>

The miniaturization of non-electronic devices did not begin as quickly as that of its electronic counterparts; it was not until the late 1970's that silicon micromachining technologies were used for the fabrication of mechanical devices. These new kinds of micro-devices were termed microelectromechanical systems (MEMS). When fluidic and optical components were developed and added to MEMS, microfluidic devices were born.<sup>6, 43</sup>

Microfluidic device fabrication grew in the 1980's when micro-sized sensors, valves, and pumps were developed and continued into the 1990's.<sup>20, 43</sup> The development of semiconductor technologies for MEMS facilitated the fabrication of complex microfluidic circuitry. Such microfluidic circuitry has also enabled chemists and engineers to multiplex and automate functions of chemical mixing, valving, separation and extraction, at the nanoliter scale.<sup>7, 13</sup>

The focus shifted in the mid 1990's to developing non-mechanical microfluidic components, such as pumps and valves that require no moving parts. The use of electromagnetic forces, electrokinetic pumping, surface tension driven flows, and acoustic streaming were all brought to the forefront.<sup>43</sup> Notably the discovery and development of polydimethylsiloxane (PDMS) soft lithography by the Whitesides group was one of the most useful advancements in proliferating microfluidic technology throughout many different scientific disciplines because it provided a simple and inexpensive method for creating microfluidic devices.<sup>26</sup>

### *1.1.2 Advantages and Applications of Microfluidic Techniques*

As fluids are reduced in scale, the physical phenomena that dominate their behavior change dramatically; on the milliliter to liter scale gravity, inertia, and convection prevail, while on the nanoliter to microliter scale viscosity, surface tension, and diffusion command fluid behavior. The physical phenomena present at the micron scale, combined with our ability to control and engineer these physical phenomena, enable many interesting studies for chemists, physicists and biologists.<sup>1, 2, 13, 15, 20</sup>

Today microfluidic devices are used in a variety of biological and analytical applications. The ability to perform chemical manipulations and analysis at the nanoliter scale has been applied to many fields where small sample volume handling and analysis is critical. Biological scientists, for instance, have a keen interest in microfluidic systems, as they require methods of analyzing and manipulating small, cell-scale, volumes.<sup>1, 2, 6, 15, 20</sup> Figure 1.1 shows several examples of microfluidic devices used for various purposes.

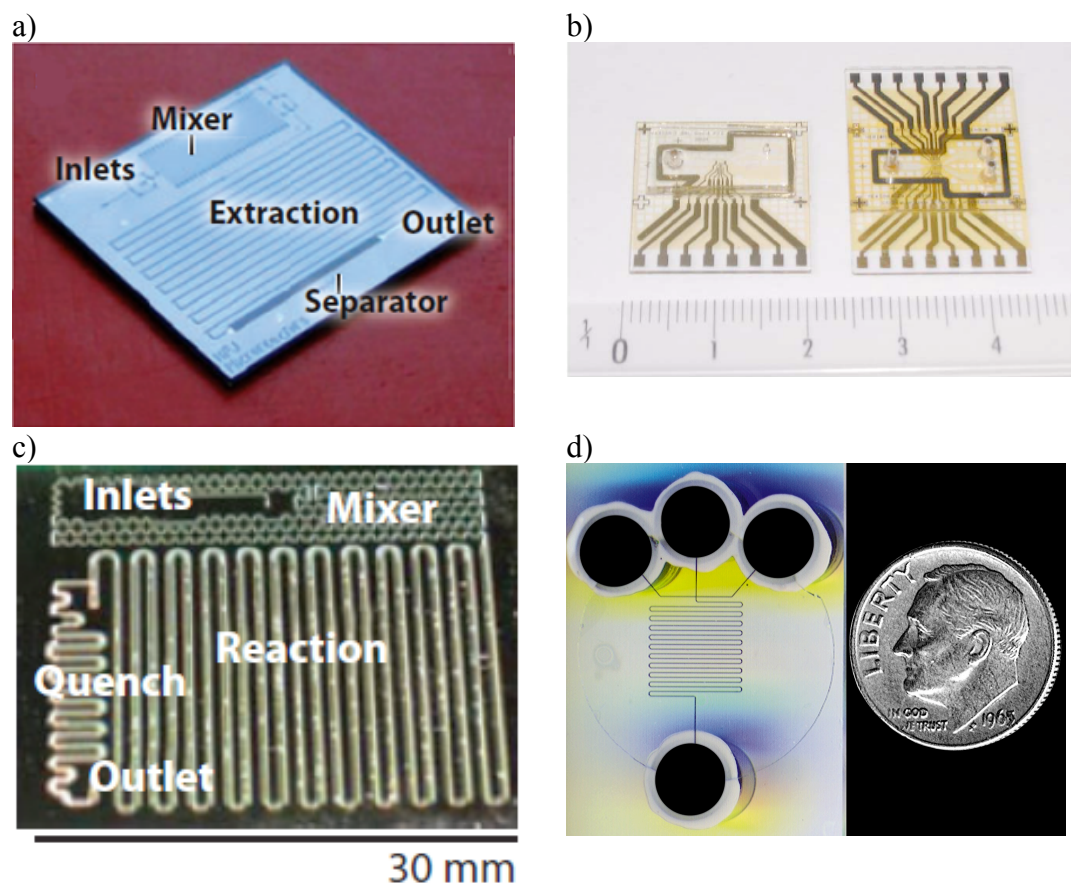


Figure 1.1 a) An integrated liquid-liquid extractor and separator<sup>46</sup> b) A PDMS microfabricated microfluidic device for cell counting and separation<sup>51</sup> c) A microreactor<sup>46</sup> d) An example of the small size of microfluidic devices

Fluid dynamics unique to the micro scale make microfluidic devices advantageous in many ways. In a practical sense, microreactors consume a much smaller volume of reagents and produce much less waste than conventional batch methods. The ability to work with small volumes is useful in reactions in which the reagents are in low supply, such as biological reactions or analyses, or when they are particularly dangerous. Microreactors can also be used with reactions



that involve moisture or air sensitive compounds or processes as the devices can isolate reactions in a closed system.<sup>2</sup>

Another important advantage of working with such small volumes is the increase in heat and mass transfer capabilities, which make microfluidic devices more efficient than batch methods. For instance, it is much easier and quicker to heat up 1  $\mu\text{L}$  of a substance by  $100^\circ\text{C}$  than it is to do the same to 1 L of a substance.<sup>3</sup> These capabilities are particularly enhanced in segmented flow systems, in which immiscible phases are separated by a distinct interface with a high surface area to volume ratio.<sup>1,6</sup> In these cases the energy and mass is transferred over a relatively large surface area.<sup>6</sup> Not only do these factors shorten the time required to change the temperature of the system and for the transfer of reagents, but it also imparts the operator with increased control over the system temperature.<sup>3</sup> Microfluidic systems such as these are able to accommodate more precise and uniform reaction times than macro-volume batch reaction methods and this has been shown to improve the reproducibility of reactions and their products.<sup>3,5</sup>

Microfluidic devices can be produced at a relatively low cost, in little time, and to suit a variety of needs. They can be used individually or in a parallel arrangement to further enhance the efficiency and output of the system. Their flexibility in design and ease of fabrication make them a promising tool for many areas of scientific research and analysis.

### 1.1.3 Flow Regimes and Regime Characterization

Flow of a continuous fluid through channels, capillary, or wide bore tubing can behave according to a laminar flow regime or a turbulent flow regime.<sup>7</sup> These two flow regimes are partly distinguished by the different mixing methods inherent in each. Turbulent flow, which takes precedence in larger scale channels, mixes its components by jostling them around. Laminar flow dominates in smaller scale systems and exhibits smooth flow that is absent of turbulence. Without turbulence, fluids can flow in parallel layers where mixing occurs primarily by diffusion, as shown in Figure 1.2.<sup>1, 2, 6, 7, 17</sup>

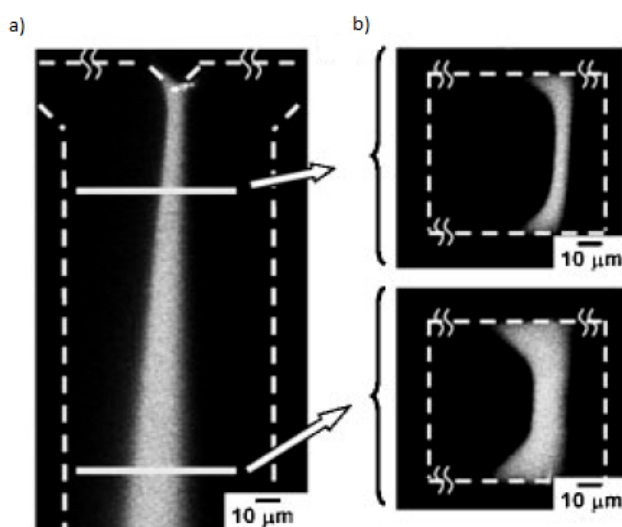


Figure 1.2<sup>22</sup> Mixing by diffusion in laminar flows. a) The inlet in the upper right corner carries a calcium containing solution and the inlet in the upper left corner carries a solution with Fluo-3, a calcium-dependent fluorophore. When mixed, they create a fluorescent complex shown by the light colored streak. The widening of the fluorescent band shows the increase in diffusive mixing as it travels farther downstream. The band is shifted to the left because calcium diffuses faster than Fluo-3. b) Vertical cross sections of the channel.

The Reynolds number ( $Re$ ) is one of several dimensionless ratios that describe various characteristics of fluid flows. The magnitude of this particular ratio is indicative of the flow regime under which the fluid is traveling, as it compares the effects of inertia to viscous stress and is given by

$$Re = \frac{Ud}{\eta} \quad (1)$$

where  $U$  is the average velocity,  $d$  is the hydraulic diameter of the channel, and  $\eta$  is the viscosity of the fluid.<sup>2, 6, 11</sup> Inertia dominates over the effects of viscosity in turbulent flow systems, where molecules are primarily transported and mixed by convection, or the net movement of the surrounding fluid. Viscous stresses dominate in smaller scale systems as they oppose inertia and turbulence in favor of moving fluids in parallel layers. This results in laminar flow where mixing occurs largely by diffusion.<sup>6</sup>

For fluids in a channel with a circular cross section, such as those used in this project, a Reynolds number of 2000 or less is indicative of laminar flow.<sup>2, 7, 17</sup> Above  $Re = 1000$  a stable sinusoidal current develops with an amplitude that increases with the flow rate until  $Re$  reaches 2000 and the transition to turbulent flow begins. Turbulent flow is completely established at  $Re = 3000$ .<sup>17, 23</sup> The smaller the dimensions of a microchannel, the more the system is governed by viscosity, and the lower the Reynolds number.<sup>6</sup>

The Reynolds number for most microfluidic systems is less than 1, as the number is directly proportional to the channel diameter which is typically on the

order of several hundred micrometers. As a result, laminar flow regimes are characteristic of microfluidic systems.<sup>7</sup> The Reynolds numbers for the microfluidic devices built in this project ranged from 0.4296 to 2.148 in capillaries with an inner diameter of 150  $\mu\text{m}$ , and from 0.2972 to 1.192 in capillaries with an inner diameter of 250  $\mu\text{m}$ , depending on the flow rates of the fluids.

Mixing and molecular transport can be described by another dimensionless ratio, the Peclét number ( $Pe$ ), which quantifies the relative importance of convection and diffusion in a system.<sup>6</sup> The Peclét number is given by

$$Pe = \frac{Ud}{D} \quad (2)$$

where  $U$  is the average velocity of the flow,  $d$  is the hydraulic diameter of the microchannel, and  $D$  is the diffusion coefficient of the molecule under consideration.<sup>2,6</sup> The smaller the Peclét number the more important diffusion is to the transport of molecules within the fluid stream.<sup>6,10</sup> The Peclét number can be adjusted by altering the fluid flow rates and the dimensions of the microchannels.<sup>6</sup> The time required for diffusion to effect complete mixing of miscible phases depends on the diffusion coefficients of the substances involved which, in turn, relies on factors such as viscosity and molecule size. If diffusion is too slow it may introduce limitations to the microreactor in cases where rapid mixing is required, such as particle synthesis.<sup>11</sup>

#### *1.1.4 Single Phase Flows in Microchannels*

Any single, continuous fluid under laminar flow conditions has a parabolic velocity flow profile when the fluids are driven by an external mechanical pressure, such as that from a syringe pump as is used in this project.<sup>1</sup> These pressure driven flows are called Poiseuille flows and can produce very high pressures within the channels—to maintain a given volumetric flow rate when the diameter of the channel decreases by a factor of 100, the applied pressure must increase by a factor of  $10^8$ .<sup>7</sup> The existence of the parabolic velocity profile means that the fluid velocity is not uniform throughout the channel, but rather that the velocity is greatest in the center of the channel and decreases radially outward towards the channel walls.<sup>1, 19</sup>

If the fluid is carrying a solute, such as growing microparticles, the non-uniform velocities will lead to dispersion of the solute, as described by Taylor dispersion and visualized in Figure 1.3.<sup>19</sup> Taylor dispersion essentially describes the broadening of a pulse of solute in a solvent stream. This phenomenon is a problem for microfluidic devices that are used as microreactors because the solute present at any given position in the channel will exhibit a range of residence times depending on the distance from the center of the channel.<sup>11</sup> Dispersion is especially problematic for the synthesis of microparticles in which a narrow size distribution is desired because particle size depends on the allowed reaction time, and wide residence time distributions correlate to wide size distributions.<sup>1, 11</sup>

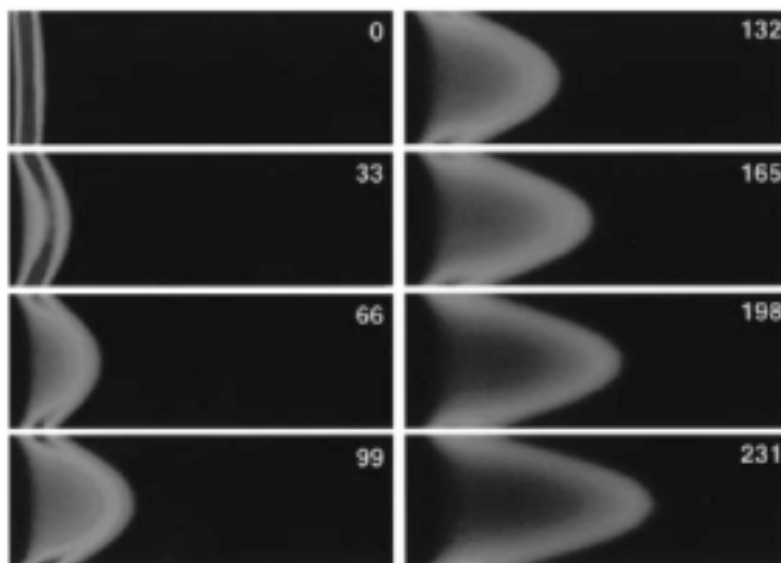


Figure 1.3<sup>7</sup> The flow profiles of a pulse of fluorescent dye in a pressure-driven system. The inner diameter of the fused silica capillaries used here are 75  $\mu\text{m}$  and 100  $\mu\text{m}$ , respectively. The frames are labeled in milliseconds after releasing the dye. In pressure-driven systems dispersion occurs because of the parabolic velocity profile of the flow.

The extent of dispersion depends primarily on capillary diameter, and to a lesser degree capillary length and flow rates. The longer the capillary the more dispersion will occur simply because the process will be carried out over a longer distance. As the flow rate is increased, the dispersion over a length of capillary will increase as well because there is a greater pressure driving the flow. Changing the diameter of the capillary, however, exerts the greatest influence on the extent of dispersion; as the diameter of the capillary decreases the degree of dispersion becomes significantly larger.<sup>23</sup>

### *1.1.5 Multi-Phase Flows in Microchannels*

#### Types of Multi-Phase Flows

A single phase system, as discussed above, consists of one or more miscible fluids flowing through a channel as a single, continuous phase. The alternative is a multiphase system which involves two or more immiscible fluids that remain distinctly separate as they flow through the channels.<sup>1</sup> There are three types of multiphase microfluidic flows as shown in Figure 1.4—wall spanning droplets, suspended droplets, and virtual walls/pinned interfaces.<sup>6</sup> In the latter two types there is a distinction between the two phases defined by the way that they behave upon interaction; the fluid that forms the droplets is considered the dispersed phase while the second fluid preferentially wets the microchannel walls and is referred to as the continuous phase, as it carries the droplets of the dispersed phase.<sup>1</sup>

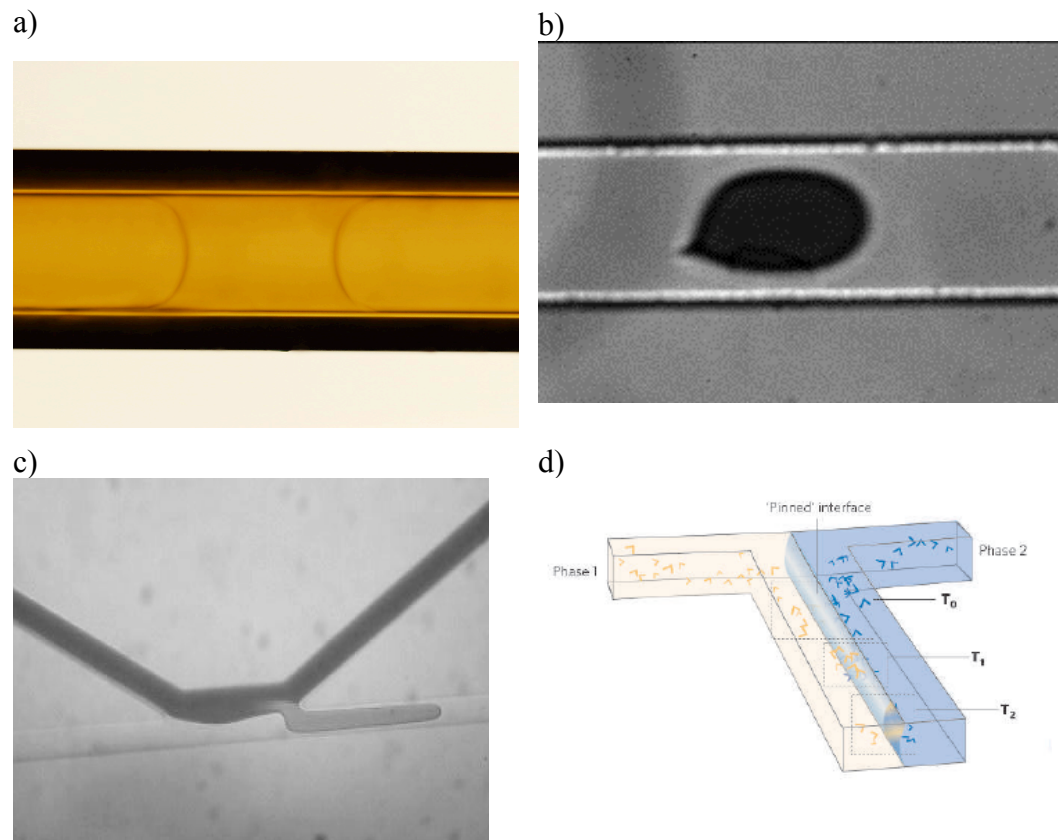


Figure 1.4 a) wall spanning droplets flanking a plug of the continuous phase b) a suspended droplet c) a pinned interface/ virtual wall multiphase flow and d) a schematic of a virtual wall system<sup>6</sup>

Wall spanning droplets are generated by the intersection of two immiscible fluids in a T-junction, the geometry of which causes the dispersed phase to break into droplets within the continuous phase. The droplets span the width of the channel, as evidenced in Figure 1.4a. This is the system of interest in this study and will be discussed in further detail shortly.<sup>6, 11, 16</sup>

Suspended droplets, as seen in Figure 1.4b are similar to wall spanning droplets in that one fluid exists as droplets dispersed in the second fluid, however, these droplets do not span the width of the channel. Instead, they are suspended



in the continuous phase and do not necessarily make contact with the channel walls. They are often produced by a flow-focusing technique, in which two streams of the continuous phase flank a stream of the dispersed phase as they are forced to flow through a narrow piece of a channel.<sup>6, 11</sup> The pressure and viscous stress exerted on the middle fluid by the flanking fluid causes it to break into droplets. This process can be carried out with nozzles or in a microfabricated device.<sup>6</sup>

Virtual walls, also called pinned interfaces, are a third type of multiphase flow and are depicted in Figure 1.4c and d. Unlike the previous two, this type does not involve droplets. Rather, it establishes a vertical interface between two immiscible fluids by patterning the channel walls to establish regional variations in the wall's hydrophobicity. Consider a multiphase system consisting of water and air as an example: The wall on the right side of the channel would be hydrophobic and the left would be hydrophilic. The water would prefer to adhere to the hydrophilic side of the channel and would remain confined to that half of the channel because of surface tension, creating a vertical interface. The formation of a vertical interface is possible on the microscale when capillarity overcomes gravitational force. Note that if macroscopic volumes of two immiscible fluids, such as oil and water, were mixed in a beaker a horizontal interface would form due to gravity and the formation of a vertical interface would be impossible. As long as the conditions within the microfluidic device are

such that capillary and interfacial stresses are dominant, a vertical interface can be formed and put to use in various extraction, reaction, and analysis procedures.<sup>6,11</sup>

### Wall Spanning Plugs and Slugs

Returning to the discussion of wall spanning droplets, the droplets can be formed with either a liquid or a gas.<sup>1, 6, 11, 16</sup> The segmenting phase is dispersed in a continuous phase that preferentially wets the microchannel. If the dispersed phase is a liquid, the droplets formed by this phase are termed “plugs”. If the dispersed phase is a gas, the droplets formed by the continuous phase as a result of the segmentation are termed “slugs”, which are of primary interest in this project.<sup>1</sup> Figure 1.5 shows examples of plugs and slugs formed in a segmented flow microreactor.

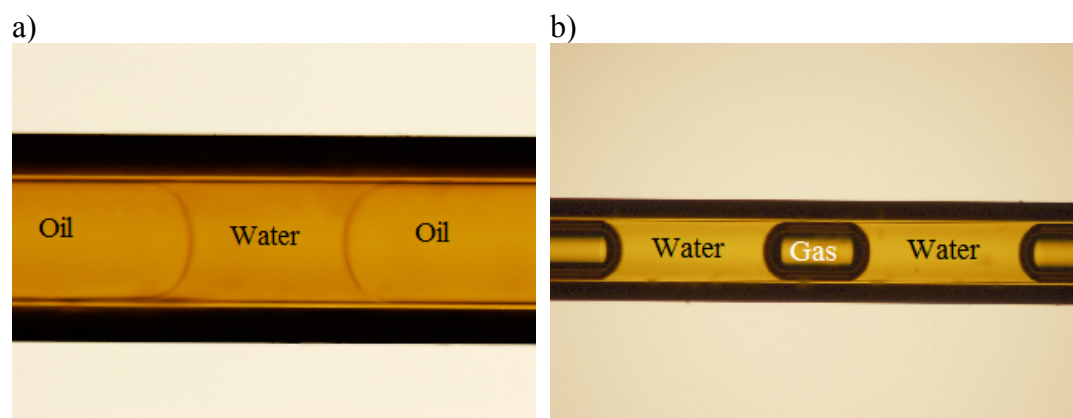


Figure 1.5. a) an oil/water wall spanning droplet segmented flow system. Oil, the dispersed phase, forms plugs because the capillary walls are hydrophilic, so water, the continuous phase, preferentially wets the walls and forms hourglass-shaped segments. b) an air/water wall spanning droplet segmented flow system. Water forms the hourglass shaped slugs separated by segments of air.

Slugs are slightly different than plugs due to their interactions with the channel walls. In hydrophilic channels, like the ones used here, the slugs preferentially wet the inner surface of the channel, producing a characteristic hour-glass shape and a thin connecting film between adjacent slugs.<sup>4,16</sup> This layer surrounds the plugs of dispersed phase and prevents them from interacting with the channel walls. The thickness of this film is reflective of the capillary number, which will be discussed shortly. Of importance here is that the smaller the capillary number, which correlates to lower viscosities and slower flow rates, the thinner the film. The same is true for the continuous phase in a system with two immiscible liquids. The film and any possibility of inter-slug contamination that it presents can be eliminated by manipulating the hydrophobicity of the channel wall and the fluids. For example, a gas-water flow in hydrophobic channels will produce discrete aqueous slugs to minimize their contact with the channel wall.<sup>4</sup>

#### Plugs and Slugs as Nano-Beakers

These plugs/slugs can be thought of as “nano-beakers”, or nanoliter sized vessels in which reactions can be carried out. When the periodicity and velocity of plug/slug translation through the channels is reproducible it allows for precise control over reaction times, giving microreactors an advantage over batch reactions. The Taylor dispersion and parabolic velocity flow profile are essentially irrelevant in segmented flows because the solutes of interest are confined within these nano-beakers.<sup>4,11</sup> Reduced dispersion, combined with a

reproducible slug size and periodicity, greatly enhances control of reaction times and produces narrower residence time distributions.<sup>10, 11</sup> Further, mixing occurs not only by diffusion within the nano-beakers but also by recirculation that is induced upon plug/slug formation. This eliminates the limitation set forth by diffusion times in single phase systems. These advantages serve to narrow the residence time and, thus, the size distribution of the product, and produce higher yields than a single phase microreactor.<sup>11</sup> Figure 1.6 shows an example of slugs that have a consistent periodicity. The discussion of multiphase flow that follows is presented as relevant to wall spanning droplets produced in a T-junction unless otherwise specified.

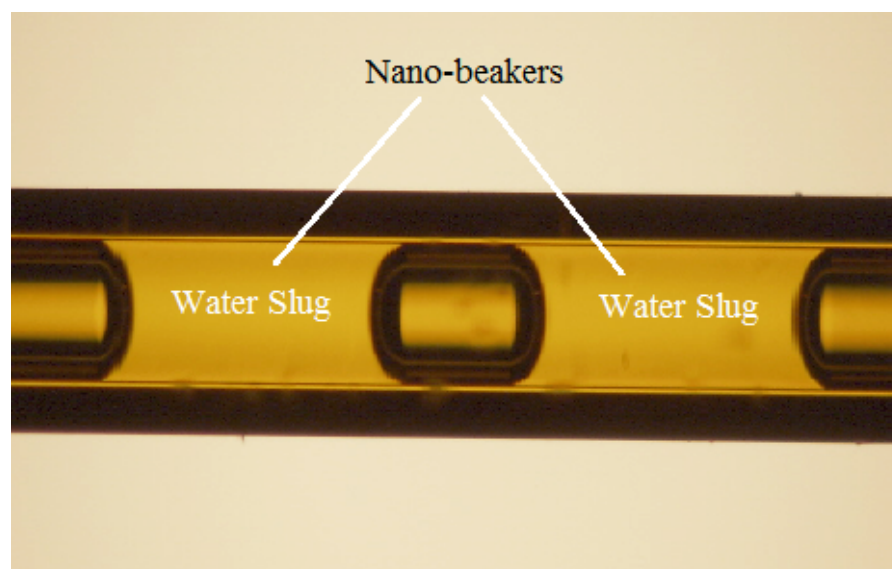


Figure 1.6. An optical microscope image of periodic segmented flow with wall spanning droplets generated in a T-junction. In this system air segmented a stream of water, producing aqueous slugs out of the continuous phase and dispersed air droplets.

### Droplet Formation

Segmentation occurs because of the presence of interfacial stresses, such as surface tension, which become increasingly important as the dimensions of the system are reduced and the surface area to volume ratio increases.<sup>1, 6, 11, 22, 23</sup>

When the diameter of the channel is less than 1 mm, interfacial stress dominates over gravitational force, as expressed by a Bond number ( $Bo$ ) of less than unity.<sup>11</sup>

The Bond number compares the relative importance of gravitational force and interfacial stress and is given by<sup>11, 20</sup>

$$Bo = \frac{\Delta\rho g d^2}{\gamma} \quad (3)$$

where  $\Delta\rho$  is the difference in density between the two immiscible fluids,  $g$  is gravitational acceleration,  $d$  is the hydraulic diameter of the channel, and  $\gamma$  is the surface tension between the two fluids. When the diameter of the channel is reduced to 1  $\mu\text{m}$ , interfacial stresses exceed gravitational force by a factor of  $10^6$ .<sup>11</sup>

Wall-spanning droplets are commonly generated by the intersection of two immiscible fluids in a T-junction, the geometry of which is shown in Figure 1.7. The continuous phase flows through the main channel, while the dispersed phase intersects the continuous phase by entering through the perpendicular channel.<sup>16</sup>

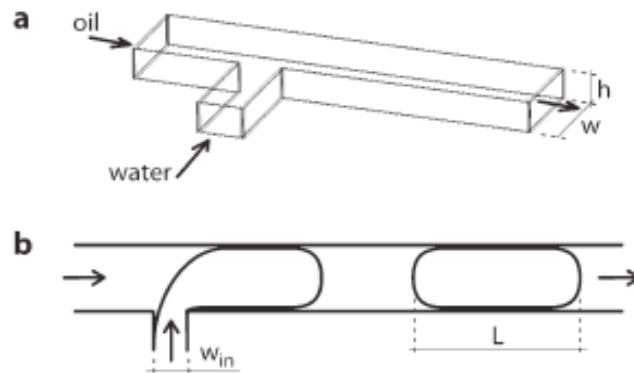


Figure 1.7.<sup>16</sup> Formation of an oil/water segmented flow in hydrophobic channels in which the oil is the continuous phase and water is the dispersed phase. a) a view of the channel geometry. b) a top view of the channel showing the formation of water plugs.

The combination of laminar flow behavior and the dominance of interfacial stress produces the plugs/slugs of segmented flow.<sup>11</sup> When two immiscible liquids merge into a single channel through a T junction there are two competing factors that drive segmentation: surface tension and viscosity. Surface tension favors the minimization of the interfacial area to minimize the surface energy. This is accomplished with the formation of plugs/slugs because the interfacial area between a plug and the continuous phase, for instance, is much smaller than the area of the interface of two linear immiscible streams that extend the length of the channel. The viscosity of the dispersed phase competes with surface tension and works to extend the interface and tow it downstream. The struggle between these two entities destabilizes the interface between the

immiscible fluids and contributes to the breakup of the dispersed stream into droplets.<sup>11, 16, 23</sup>

The capillary number ( $Ca$ ) describes the struggle between viscous and interfacial stresses in microfluidic systems. It is given by

$$Ca = \frac{U\eta}{\gamma} \quad (4)$$

where  $U$  is the velocity of the dispersed phase,  $\eta$  is the viscosity of the continuous phase, and  $\gamma$  is the interfacial surface tension between the phases.<sup>4, 6, 11, 23</sup> In order to form plugs/slugs the capillary number must be low. The interfacial surface tension,  $\gamma$ , must be great enough to encourage the formation of droplets to minimize the interfacial area, and the viscosity of the dispersed phase must not be too great as to inhibit the formation of droplets.<sup>16</sup> The capillary numbers of segmented flow systems constructed in this project ranged from  $1.92 \times 10^{-4}$  to  $7.71 \times 10^{-4}$ . These values are well below  $10^{-2}$ , which is usually the upper limit of  $Ca$  for microfluidic systems.<sup>16</sup>

Because the capillary number is small, shear stress exerted on the dispersed phase as it enters the main channel is also small and is overcome by interfacial stresses and surface tension.<sup>16</sup> This allows the dispersed phase to span the width of the main channel before a droplet is severed from the stream, leading to the formation of wall spanning plugs/slugs. Only a thin layer of the continuous phase separates the dispersed phase from the main channel walls. The blocking of the continuous phase stream by the dispersed phase creates a heightened pressure

upstream of the forming droplet, which effectively squeezes the dispersed phase stream until the droplet breaks off and the tip of the stream retracts back into the inlet channel before the process begins once more.

The magnitude of the pressure and, therefore, the rate at which droplets are formed can be controlled by adjusting the flow rates of the phases. By adjusting the rate at which plugs/slugs are formed their volume is also adjusted. Additionally, the dimensions of the channel affect plug/slug volume, periodicity, and the mechanism of breakup. As the dimensions of the channel decrease the volume of plugs/slugs decreases, while their periodicity increases. Effectively, as the channel diameter decreases there will be more plugs/slugs within a certain channel length and they will have a lower volume.<sup>11, 16</sup>

Droplet size is related to the capillary number by

$$R \sim \frac{h}{Ca} \quad (5)$$

where  $R$  is the radius of the plug/slug and  $h$  is the height of the channel. This equation comes from the ratio of interfacial to viscous stresses that also defines the capillary number itself. Interfacial stress ( $I$ ) is represented by

$$I = \frac{\gamma}{R} \quad (6)$$

and viscous stress ( $V$ ) is represented by

$$V = \frac{U\eta}{h} \quad (7)$$

where all variables retain the same representation as in Equation 4.<sup>11,23</sup> The ratio of interfacial stress to viscous stress gives



$$\frac{I}{V} = \frac{h\gamma}{U\eta R} = \frac{h}{CaR} \quad (8)$$

when  $Ca$  is defined as it is in Equation 4. The quantifiable relationship between viscous and interfacial stresses allows for the production of reproducible plugs/slugs to be used as nano-beakers.<sup>23</sup>

### Mixing

Mixing can occur relatively slowly in single phase laminar flow regimes because it is due primarily to diffusion. Several methods of supplemental mixing have been applied to microfluidic systems in attempts to improve mixing by reducing both the diffusion time and distance.<sup>7</sup>

Segmentation is one of these methods and is considered a passive form of mixing.<sup>2</sup> The process of forming the plugs/slugs as well as surface tension differences between phases initiates recirculation in the nano-beakers.<sup>1, 2, 5, 10</sup> Figure 1.8 shows an image of the 2D velocity vectors produced by recirculation within a slug. Segmentation also improves the speed and efficiency of mixing by reducing the diffusion distance since a shorter diffusion distance shortens the time scale associated with mixing by diffusion.<sup>10, 11</sup>

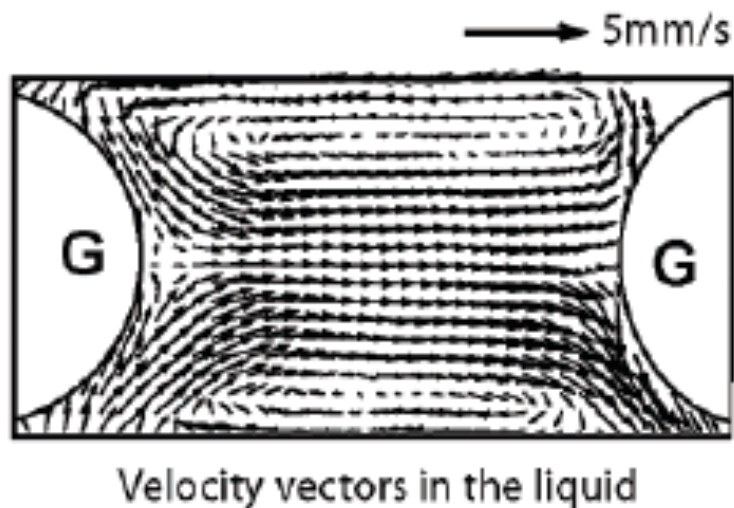


Figure 1.8.<sup>10</sup> Velocity vectors of recirculation in a plug produced with segmented flow.

Passive mixing in plugs/slugs can also be enhanced by chaotic advection. This process involves the incorporation of a winding micro-mixing segment built into the microfluidic device. As the plugs travel around a corner or turn its contents are folded into layers. The result of several repetitions of this mixing effectively reduces the diffusion distance and the mixing time.<sup>1</sup> The same effect can be produced with patterned microchannel walls.<sup>10</sup> Figure 1.9 shows an example of chaotic advection from patterned walls.

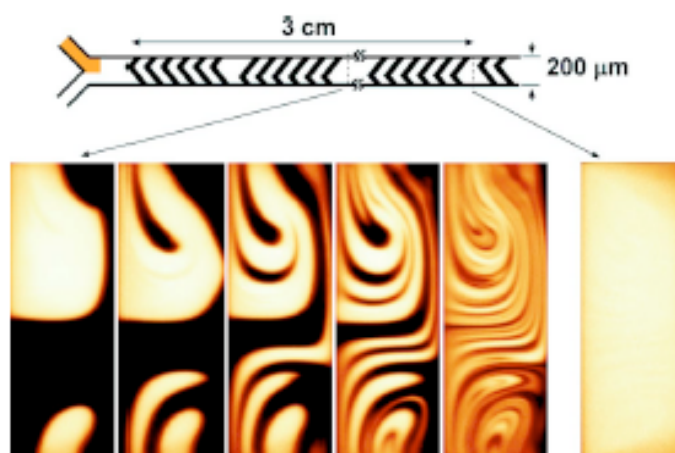


Figure 1.9.<sup>23</sup> Chaotic advection induced by herringbone-patterned channel surfaces.

The mixing time and method is an important consideration for microreactors, especially in the synthesis of particles, because the extent of mixing and reaction time determines the size and morphology of the particles formed.<sup>5</sup>

## 1.2 Fabrication and Operation of Microfluidic Devices

### 1.2.1 *Microfabricated Devices*

Microfabrication produces devices in which the entire channel network is contained on a substrate with an area of a few square inches. These devices can be made with either two- or three-dimensional channel networks and can include

various inlet and outlet channels, microwells, and winding channels that facilitate mixing.<sup>43</sup>

Microfabrication techniques include photolithography, micromachining, and soft polymer lithography. Early in the development of microfluidics, devices were created using photolithography to delineate a channel network on a silica substrate. Silica was eventually replaced by glass because the latter made for easier visualization of activity inside the device and remains the dominant method today.<sup>20</sup>

### Photolithography

Photolithography is a top down method of microfabrication that is used to create microfluidic devices. It involves the chemical modification of areas on a layer of photoresist that change its solubility in a specific solvent. The chemical modification is achieved by irradiating the photoresist with high frequency radiation, like UV light.<sup>9, 42, 47</sup> Typically, a layer of photoresist is spin coated onto a substrate and is subsequently covered with a photomask. The photomask is a transparent, non-absorbent piece of glass or plastic that bears the desired channel design in a UV-absorbent material.<sup>42</sup> When made of thin plastic they can be created with a computer aided design (CAD) program and printed on a printer with a resolution of about 20  $\mu\text{m}$ .<sup>26, 28</sup>

The substrate, photoresist, and photomask are exposed to the beam of radiation. Any photoresist that is not protected by the channel design undergoes a

light-catalyzed reaction that causes the change in its solubility, usually by either polymerization or chain scission. Chain scission generally improves the solubility of the resist, while polymerization decreases its solubility.<sup>9, 48</sup>

If the solubility of the photoresist improves upon irradiation it will be dissolved in the appropriate developer solution, leaving only the un-modified resist in the pattern of the channel design on the substrate. This type of photoresist is a positive photoresist. Alternatively, if the solubility of the photoresist worsens upon irradiation the un-modified photoresist will dissolve in the appropriate developer, leaving a negative image of the channel design in the remaining photoresist. This type of photoresist is a negative photoresist. These distinctions are presented in Figure 1.10.<sup>9, 47</sup>

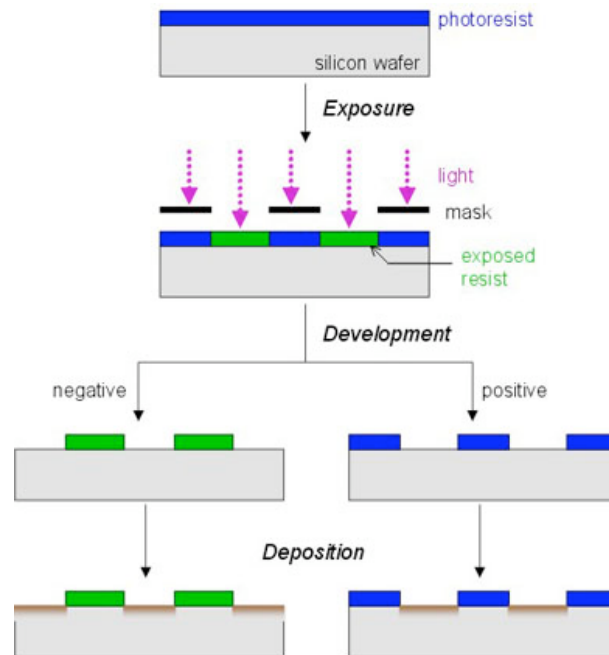


Figure 1.10.<sup>53</sup> The process of photolithography to produce a negative or positive photoresist

Poly(methylmethacrylate), PMMA, is a commonly used positive photoresist. Upon irradiation by deep ultraviolet light, PMMA becomes soluble in basic developer solutions after undergoing chain scission as shown in Figure 1.11.<sup>48</sup>

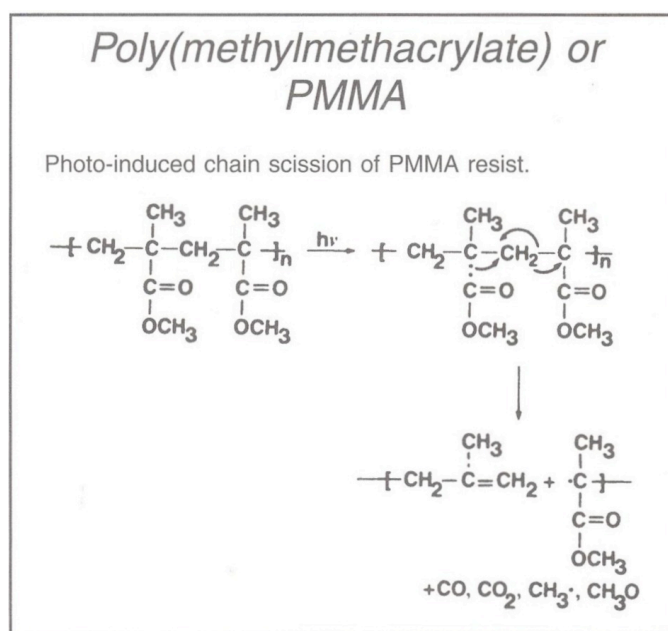


Figure 1.11.<sup>48</sup> The light catalyzed chain scission reaction of PMMA, a positive photoresist. Chain scission increases its solubility in a basic developer allowing for the removal of all photoresist except for that in the pattern of the channels.

The substrate will bear the pattern of the desired microchannels as either a positive or negative resist, and this can be etched onto the silicon wafer to create a microfluidic device or used as a master to mold a polymer-based device.<sup>48</sup>

### PDMS Soft Lithography

Glass was replaced in the early 1990's by polydimethylsiloxane (PDMS) when George Whitesides' group introduced soft lithography as a method of microfluidic device fabrication.<sup>20, 27</sup> It involves the use of a mold to create microchannels in a polymer, such as PDMS, which are then cured and bound to a substrate to seal the channels and enclose the system. Soft lithography is a popular method of device fabrication for several reasons, primarily due to the fact that it is a relatively inexpensive and faster process compared to photolithography or micromachining. It also requires less technical expertise, yet offers a greater flexibility in channel designs than the alternatives.<sup>28</sup>

Soft lithography begins with the creation of a master which is then used itself as a mold for the device, or to make a polymer mold. The master is made by photolithography, as described above, so that a photoresist such as SU-8 or PMMA, is patterned on a silica wafer in the desired channel design.<sup>13, 16, 28</sup> The resulting master is then covered in PDMS precursor solution and cured for one hour at 70-80°C. PDMS is an elastomeric solid polymer that is made by combining an elastomeric silicon polymer base with a cross-linking solution.<sup>27,28</sup> After the polymer is cured it can be peeled off of the master, leaving the channel pattern embedded in the PDMS.

The patterned PDMS can be sealed to a glass slide or another piece of PDMS to enclose the channels by oxidizing both surfaces with a plasma gun and

gently pressing them together. This creates an irreversible seal between the two pieces.<sup>26, 28</sup> Figure 1.12 shows a schematic of the soft lithography process.

Although silica and glass are slightly superior to PDMS in terms of chemical resistance and mechanical, thermal, and optical properties, the ease and low cost at which PDMS microfluidic devices can be produced make them popular.<sup>20</sup> PDMS soft lithography is the prevailing method of microfluidic device fabrication today.<sup>20, 28</sup>

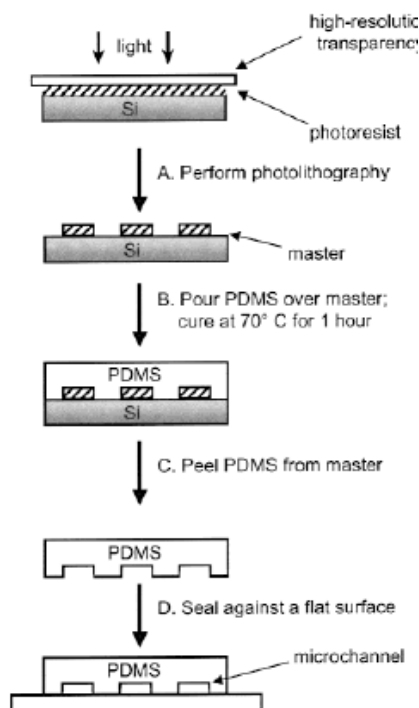


Figure 1.12.<sup>28</sup> The soft lithography microfabrication process to produce a PDMS microfluidic device

### 1.2.2 Microfluidic Devices Constructed with Commercially Available Fluidics

It is possible to use commercially available fluidics and materials, such as T-junctions and capillaries, to construct microfluidic devices that operate under



the same principles and produce the same results as those devices constructed via top-down methods. This method of microreactor construction is particularly advantageous because of the ease with which it can be put together and be repaired, and it lacks the long work times and instrumentation required for the creation of microfabricated devices. This project represents the first time that a microreactor built with commercially available capillary fluidics has been used to synthesize microparticles in a segmented flow regime. Figures 1.13 and 1.14 show images of the single phase and segmented flow commercially-based microreactors built and used in this project.

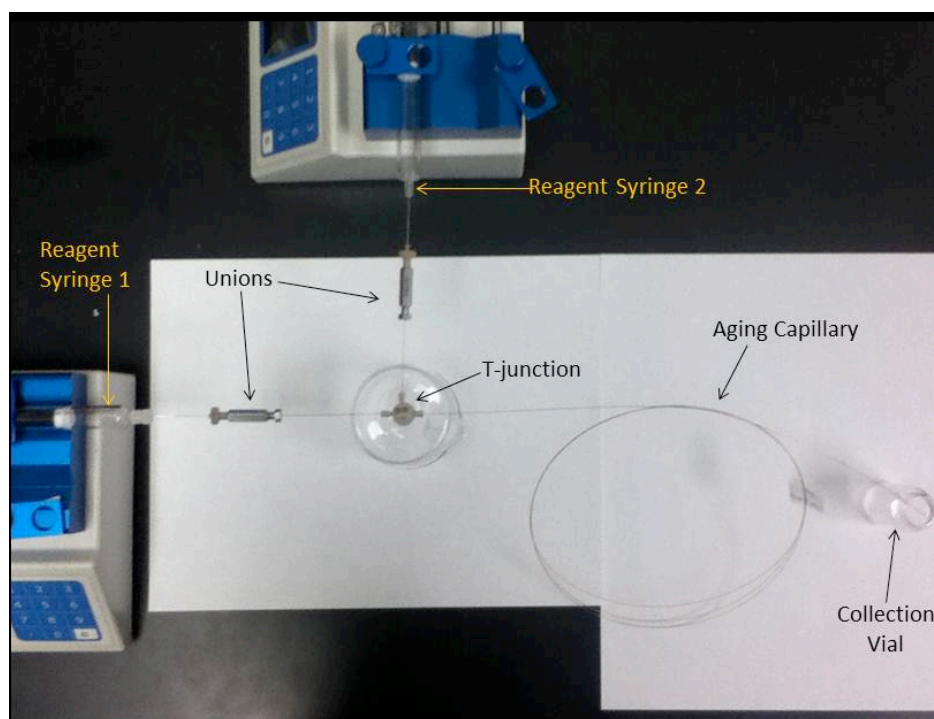


Figure 1.13. The single phase microreactor used in this experiment

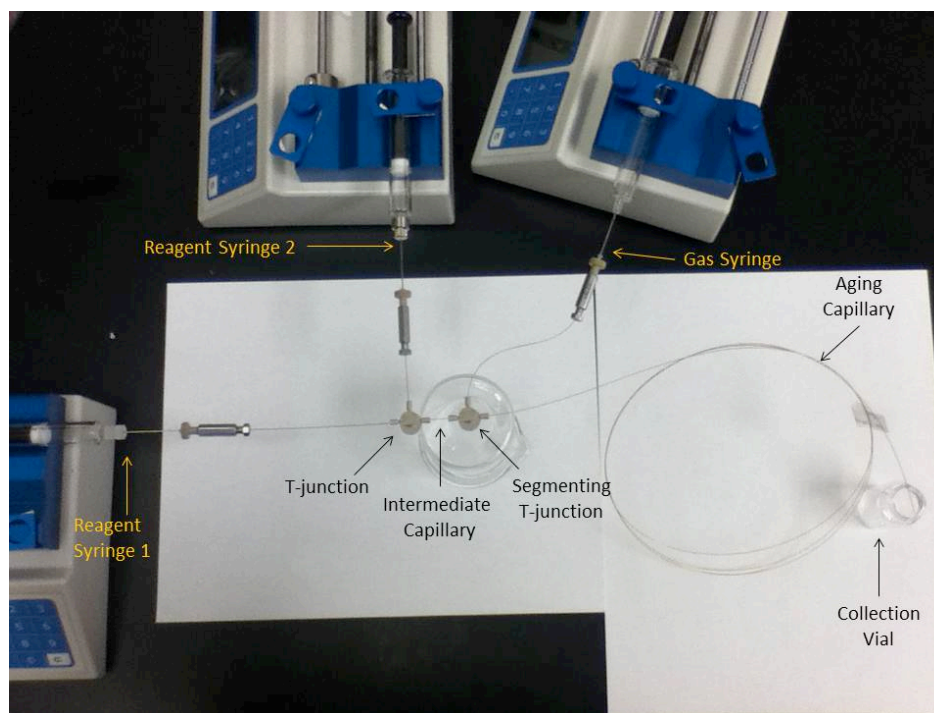


Figure 1.14. The segmented flow microreactor used in this experiment

### Commercially Available Fluidics

Flexible fused silica capillary tubing is available with a variety of inner and outer diameters and can serve as microfluidic channels in a commercially based microfluidic device. This capillary tubing can be purchased from Polymicro Technologies with a circular cross section with inner diameters ranging from 2 to 700  $\mu\text{m}$  and outer diameters from 150 to 850  $\mu\text{m}$ . The outer surface is covered in a polyimide coating that is able to withstand temperatures of up to 350°C. Other varieties of capillary are also available, such as that with a square cross-section, and coatings that withstand higher temperatures or are UV-transparent.<sup>49</sup>

T-junctions, such as that shown in Figure 1.15, are available from manufacturers such as Valco Instruments Co. Inc. There are many designs available and all are suited for different purposes; different styles can withstand varying degrees of pressure, have different internal and external geometries, and are made for different volumes. Tees are available in a variety of metals including an inert plastic, polyetheretherketone (PEEK), which is biocompatible and metal-free. Of particular interest for commercially based microfluidic devices are PEEK tees designed to join with capillary with a 360  $\mu\text{m}$  outer diameter. This type of tee is available with a number of different inner diameters, from 50 to 150  $\mu\text{m}$ , and is able to withstand a pressure of up to 10,000 psi.<sup>50</sup>

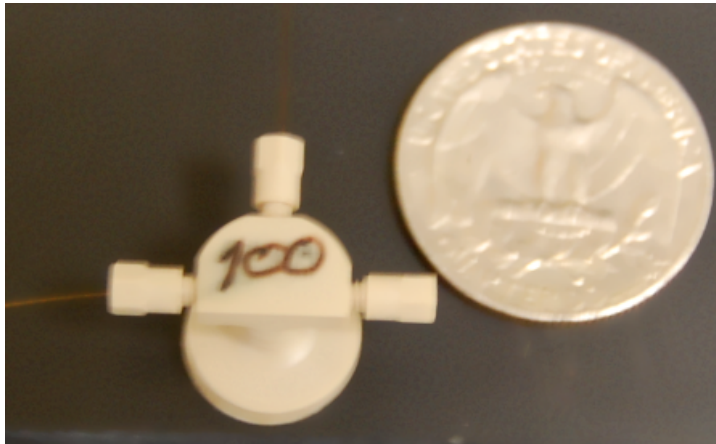


Figure 1.15. A microfluidic T-junction with an inner diameter of 100  $\mu\text{m}$  is slightly smaller than a quarter

A union is needed to join the end of a capillary with the syringe containing the fluid to be pumped into the microreactor. These are often made of steel, or a combination of steel and PEEK, as shown in Figure 1.16.<sup>50</sup>



Figure 1.16. A steel and PEEK union connecting the needle of a syringe to a capillary

The method of constructing microfluidic devices with commercially available fluidics has its advantages, particularly in terms of troubleshooting operational problems. Although commercially-based devices take up more space than microfabricated devices and are limited to relatively simple channel features and patterns, they tend to be much easier to troubleshoot and can accommodate a wide range of residence times. For instance, a clogged capillary can be remedied

by simply replacing that piece of capillary with a fresh piece, while a clogged channel in a microfabricated device may necessitate remaking an entirely new device, adding hours of extra work. Capillary-based devices can be adjusted to suit nearly any residence time required of it by selecting the necessary length for the aging capillary. Microfabricated devices are somewhat limited in this respect as the aging channel must be able to fit on the small device. This method of design also makes for easier flow characterization under a microscope as only a piece of the capillary needs to be run across the microscope stage as opposed to an entire micro-fabricated device.

#### Capillary Fabrication

The merging of fiber optics fabrication and microelectronics technologies made the manufacturing of small bore fused silica capillaries possible. The process begins when a synthetic silica tube is fed into a graphite furnace at a temperature of 2000°C. The silica melts and is drawn down by the capstan at a controlled speed, anywhere between 3 and 40 m/min, that will produce the desired capillary dimensions. As it is drawn down it is coated with up to six layers of polyamic acid, each of which are dehydrated prior to adding another layer, to produce a polyimide coating on the bare glass. This coating increases the strength and durability of the capillary and helps to protect it from breakage.<sup>24</sup>

A micrometer monitors the outer diameter of the bare glass tube and the cured coating diameter with two lasers. These measurements allow for the

detection of flaws and non-circularity in the capillary, as well as a recording of the minimum and maximum dimensions. The synthetic silica tubes initially fed into the furnace are not free from defects themselves and these imperfections can be translated to the capillary causing non-uniform polyimide coatings, non-circular geometries, variation in capillary diameter, and a lack of concentricity between the inner and outer diameters, to name a few. Figure 1.17 shows a possible design schematic for a drawing and coating machine.<sup>24</sup>

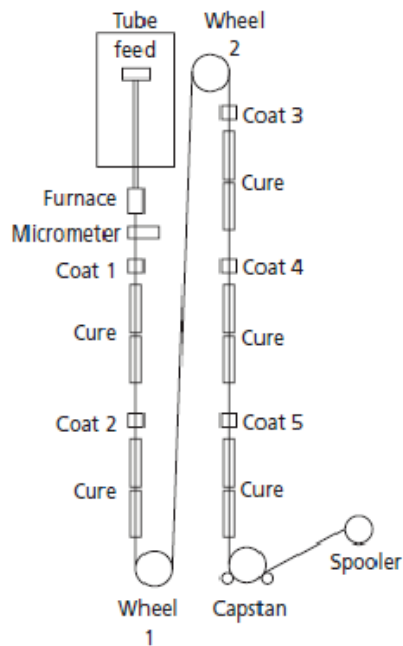


Figure 1.17<sup>24</sup>. Possible arrangement of a drawing and coating machine for fused-silica capillary production

#### 1.2.4 *Ancillary components*

##### Pumps and Syringes

In order to put a microfluidic device to use, there must be a force moving the fluids through the microchannels. For pressure driven flows this is often provided in the form of a syringe pump.<sup>7</sup> The syringe pump allows the user to control the fluid flow rates. Syringes are connected to the device by a capillary that connects to the syringe with steel or steel/PEEK unions, as shown in Figure 1.16 above. Syringes loaded with fluids are placed on the syringe pumps and expelled at programmed rates.

The type of syringe is important; it must be capable of withstanding the high pressures associated with microfluidic systems and it must be gastight if gas is being used to segment the flow. A blunt needle tip makes the best connection inside of the union. If the tip is beveled leaking may occur, particularly if the syringe is injecting gas into the device.

##### Microscopes

Flow can be visualized with optical microscopes by placing all or part of the microfluidic device on the microscope stage. Bright field light microscopes illuminate the sample with an incandescent bulb.<sup>11, 21</sup> This method is relatively simple to use and suited for samples that are able to absorb light. Samples must have some sort of pigmentation and be of an adequate thickness to have the ability to absorb light. Bright field microscopy generally produces good results,

although the images can lack contrast. Dark field microscopy only allows light that is scattered by the sample to be seen by the operator. This restriction makes it possible to image objects that cannot be seen under bright field conditions because they are too thin or have no absorbance. Dark field microscopy requires a greater light intensity than bright field microscopy, but does have the benefit of illuminating very small or non-absorptive objects.<sup>21</sup> Additionally, a digital camera is often fitted to the microscope so that still images and movies of the flows can be captured.<sup>11</sup>

#### Heaters and Coolers

Some form of temperature control is often needed for a particular reaction or analysis scheme. Heating and cooling elements can be integrated into microfabricated devices to contribute to the consolidation of an entire reaction or analysis scheme onto a single, small device. Thin film heaters have been integrated into lab-on-a-chip devices for DNA analysis and can span the entire microfluidic network, or only a part of it, or create different temperature zones.<sup>51</sup>

A common source of thermal control is a Peltier thermoelectric device that can pump heat from one surface to another.<sup>52</sup> One or more of these units can be placed beneath the substrate and can either heat or cool the system, as well as create temperature gradients.<sup>12</sup> For capillary based microfluidic systems a simple hot water bath is an easy way to create an elevated temperature zone.



### 1.3 Experimental Methods—Characterization of Segmented Flow

Silica and titania microspheres were synthesized in three different reactors: a batch reactor, a single phase microreactor, and a segmented flow microreactor. Before synthesis was carried out, however, these reactors had to be built and the flows produced by the segmented flow microreactor had to be characterized.

#### *1.3.1 Construction of the Reactors*

Three different reactors were used to synthesize ceramic microspheres: a single phase microreactor, a segmented flow microreactor, and a batch reactor.

The single phase microreactor was assembled as shown in Figure 1.18. Two gastight syringes (Hamilton, 1700 series, Reno) on syringe pumps (Chemyx, Fusion 100, Stafford, TX) were used to inject reagents into the capillary network. Capillaries with a circular cross section and 150  $\mu\text{m}$  inner diameter (ID) were joined to each of the two syringes with steel unions (Valco Instruments, Houston). The capillaries carried the reagents to a 150  $\mu\text{m}$  ID microfluidic T-junction (Valco Instruments, Houston) where the reagents combined and travelled into the aging capillary of variable length and an inner diameter of either 150  $\mu\text{m}$  or 250  $\mu\text{m}$ . The products were collected at the end of the aging capillary in a vial.

The segmented flow microreactor was constructed in a similar way, differing only by the addition of a second T-junction and an inlet capillary for air to segment the reagent stream. The device is shown in Figure 1.19.

The batch reactor was simply a scintillation vial in which the reagent solutions were mixed.

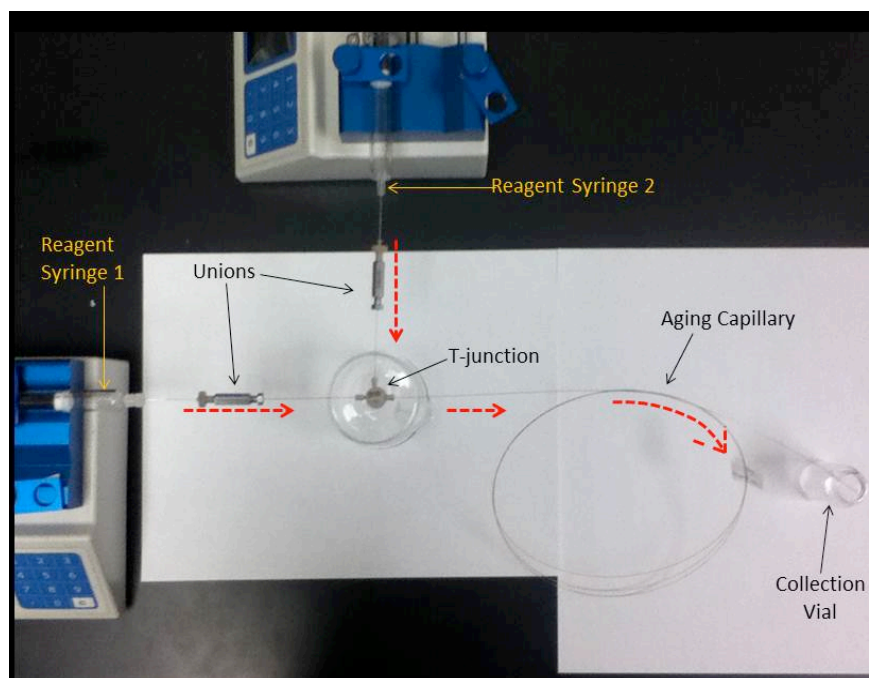


Figure 1.18. Single phase microreactor. The dashed lines indicate the flow path of the reagent streams.

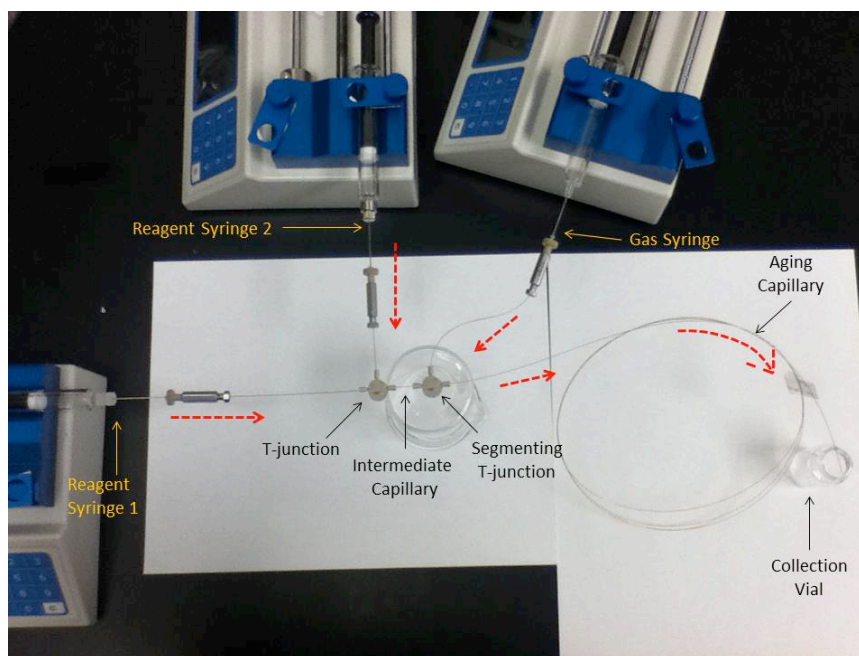


Figure 1.19. The segmented flow microreactor constructed for this experiment. The dashed lines show the flow path of the fluids in the system

### 1.3.2 Characterization of the Segmented Flow Microreactor

A segmented flow of wall spanning plugs was generated in the segmented flow microreactor with water and perfluorodecalin (PFD) as the two immiscible phases. The water was dyed with green food coloring to distinguish it from the PFD. The volume of the aqueous plugs produced by the segmented flow microreactor were characterized by capturing images and movies of the flow at 100x magnification on a light microscope (Olympus, Bx51, Center Valley, PA) with an digital camera (Olympus, DP70, Center Valley, PA). The average plug volume and the average rate of plug formation were analyzed for water flow rates between 0.05  $\mu\text{L}/\text{min}$  and 0.5  $\mu\text{L}/\text{min}$  with a constant PFD flow rate of 0.25

uL/min. Likewise, these averages were calculated for PFD flow rates between 0.05 and 0.35 uL/min with a constant water flow rate of 0.125 uL/min.

The average plug volume of each flow condition was determined through image analysis of three images for each flow rate with Igor Pro, which calculated the plug length in pixels so that it could be converted to a volume measurement. The average volume values were then plotted against the flow rates.

Image analysis was done using Igor Pro, in which images taken on the microscope were imported into the program and analyzed with an image line profile. The image line profile displayed the RGB levels of the image along a selected horizontal line. The interfaces between phases were distinguished by a sharp drop in the RGB levels as the color of the image was much darker at these interfaces. The length in pixels between interfaces was recorded and converted to the desired units. Figure 1.20 shows an example of an image and its line profile.

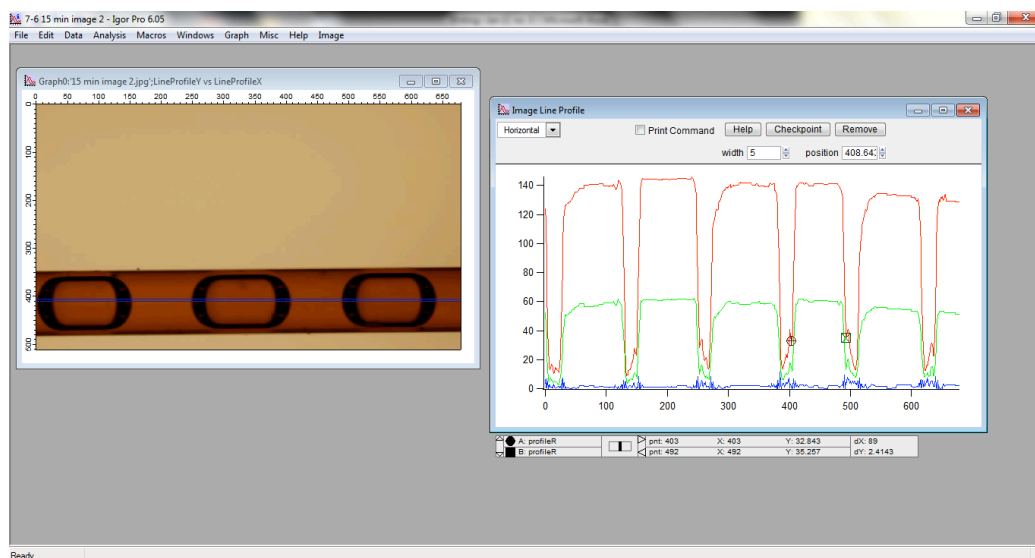


Figure 1.20. Igor Pro Image Line Profile. The sharp changes in the RGB levels indicate the interfaces at the edges of the plugs.

The average rate of plug formation was determined by viewing three movies of the flow at each of the flow rates. For each movie, the number of plugs that passed through the viewing area in one minute were counted and averaged. The rates in units of plugs per minute were converted to units of plugs per second. The rate of plug formation should be distinguished from the plug velocity—the rate of plug formation is the number of plugs produced in a given amount of time and the intervals between them, while the plug velocity is the distance that a plug travels in a given amount of time. The rate of plug formation is a crucial measurement when using a microfluidic device as a microreactor, as it is a consistent periodicity of plugs that provides precise control over the extent and duration of a reaction.

#### 1.4 Results and Discussion

The inner surface of the capillary is hydrophilic. Figure 1.21 shows an image of the segmented flow, where the dark colored water plugs behave as the continuous phase and preferentially wet the capillary wall. Consequently, any aqueous reaction performed in the microreactor takes place in these aqueous plugs.

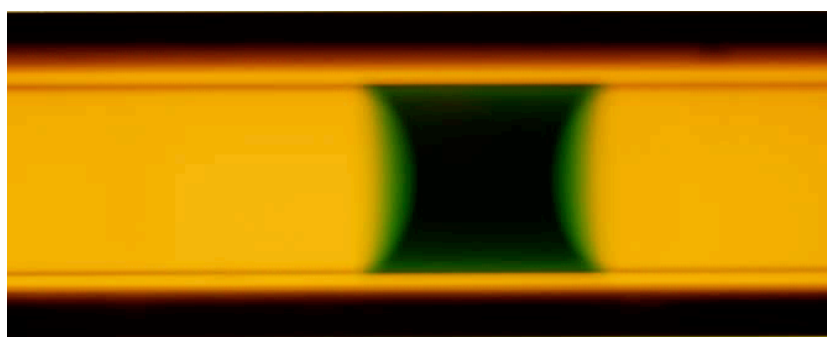


Figure 1.21. Wall spanning plugs in the segmented flow microreactor. The light colored plugs are PFD and the dark segments are water. Because the water segments preferentially wet the capillary wall it can be concluded that the capillary walls are hydrophilic.

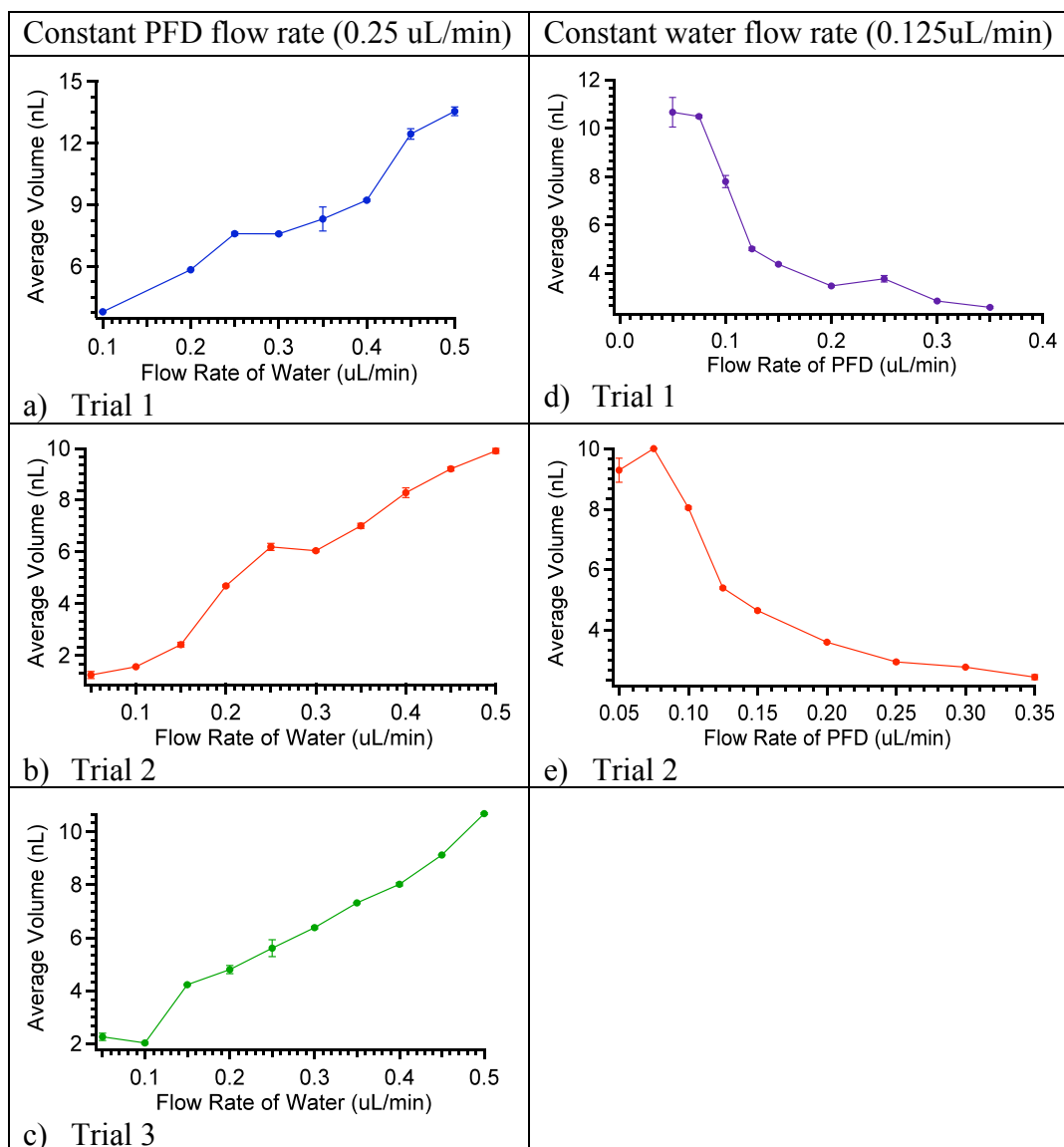


Figure 1.22. Average volumes of aqueous plugs under different phase flow rates. a, b, and c represent constant PFD and changing water flow rates, while d and e represent constant water and changing PFD flow rates.

Figure 1.22 shows the effect that changing either the PFD or water flow rate has on the volume of the aqueous plugs: an increase in the flow rate of the water stream increases the volume of the aqueous plugs, while an increase in the

flow rate of the PFD stream decreases the volume of the aqueous plugs. This makes sense because the faster the water stream is flowing the more volume will be contributed to a forming plug before a PFD droplet intercepts the stream. Similarly, when the PFD stream is flowing fast the PFD droplets form more quickly and, therefore, intercept the water stream more frequently.

Water flow rates slower than about 0.25  $\mu\text{L}/\text{min}$  generated plugs of somewhat unpredictable volumes, just as PFD flow rates slower than about 0.1  $\mu\text{L}/\text{min}$  did the same. These observations, however, could be indicative of incomplete equilibration of the syringe pumps rather than the mechanics of droplet generation.

Plugs with volumes ranging between about 2 and 12 nL were generated under different flow conditions. The largest standard deviation in plug volume in all of the constant PFD trials is only 0.58 nL, with most of the standard deviation values measuring less than 0.1 nL. For the constant water trials the largest standard deviation was 0.61 nL, although the majority still had a standard deviation of less than 0.1 nL. This confirms that the aqueous plugs generated for each set of flow rates were of uniform size. Further, the plug volume exhibits little variation between trials aside from several outliers, which speaks to the reproducibility of the plugs.



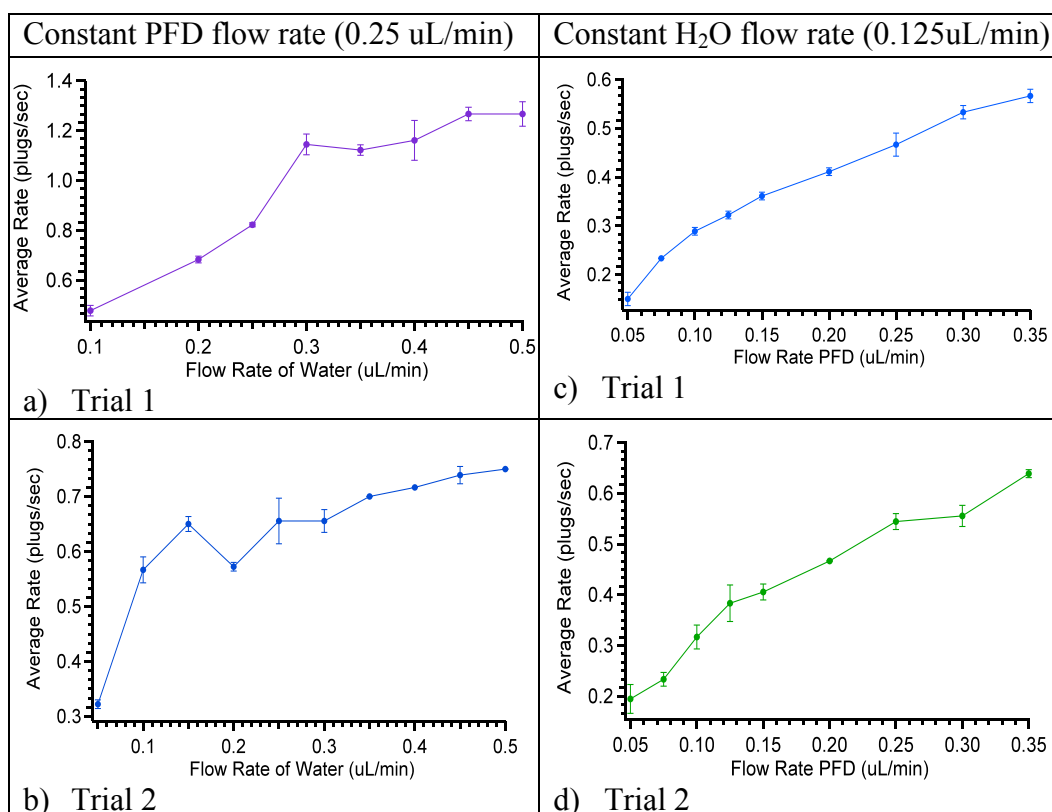


Figure 1.23. Average rates of aqueous plug flow under different phase flow rates. a and b represent constant PFD and changing water flow rates, while c and d represent constant water and changing PFD flow rates.

Figure 1.23 shows the rate of aqueous plug flow for water flow rates between 0.05 and 0.5 uL/min with a constant PFD flow rate of 0.25 uL/min, as well as the rate of aqueous plug flow for PFD flow rates between 0.05 and 0.35 uL/min, with a constant water flow rate of 0.125 uL/min. Average rates between 0.15 and 1.27 plugs/sec were produced. The rate of aqueous plug flow generally increases with an increase in either the water or PFD flow rate.

The greatest standard deviation in the average rate is 0.079 plugs/sec in Trial 1 of the constant PFD trials. The standard deviations for the remaining trials all fall below 0.37 plugs/sec. Low standard deviations in the rate of plug flow

indicate that the flow has consistent and reproducible periodicity. It is this characteristic of segmented flow systems that allows for enhanced control over the reaction time and makes microreactors an excellent device to use for the synthesis of microparticles, whose size and polydispersity depend on consistent reaction times.

## CHAPTER 2—SOL-GEL SYNTHESIS OF CERAMIC MICROSPHERES

### 2.1 Introduction to Sol-Gel Chemistry

#### *2.1.1 Reproducible and Monodisperse Ceramic Microspheres*

Microspheres are particles with diameters measuring between hundreds of nanometers and microns. In the past several decades they have become increasingly popular as a widely applicable new technology in areas including medical imaging and drug delivery, construction materials, renewable energy, and chromatography, to name a few. They are often advantageous over bulk materials with the same chemical composition because they have high surface area to volume ratios and their surface chemistry can be engineered.<sup>33, 34, 35, 37</sup>

Microspheres can be synthesized from a variety of materials including alumina, silica, titania, and other metal oxides.<sup>35</sup>

Monodispersity and reproducibility are highly coveted qualities of microspheres. Monodispersity, or a narrow size distribution, eliminates the variable introduced by a wide size distribution and allows for more accurate interpretations of experimental results.<sup>35, 39</sup> In chromatography, monodispersity allows for the peak capacity and efficiency of packed columns because monodisperse particles can be packed with less void volume than a relatively polydisperse solution. Suspensions of monodisperse microspheres are also needed for use as calibration standards for analytical instrumentation.<sup>39</sup> Monodispersity

is difficult to achieve by batch synthesis procedures because the reaction time and, therefore, particle size, is difficult to precisely control in this method.<sup>3, 5</sup>

Reproducibility is equally important and relates to a narrow size distribution between separate synthesis trials. In order to be able to produce microspheres of specific sizes the method used to synthesize them must consistently generate similarly sized microspheres under a given set of reaction conditions. This allows for size tunability and is important for industrial microsphere production.<sup>3</sup>

Silica and titania, formally named silicon dioxide ( $\text{SiO}_2$ ) and titanium dioxide ( $\text{TiO}_2$ ), respectively, are ceramics that can be easily synthesized in the form of microspheres via sol-gel chemistry. Silica, in particular, is a very popular option for microsphere synthesis and is the model system for the study of sol-gel chemistry.<sup>31, 35</sup> An SEM image of silica microspheres can be seen in Figure 2.1.

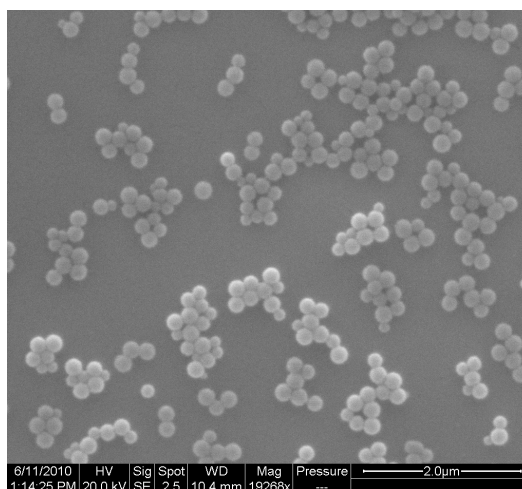


Figure 2.1. An SEM image of silica microspheres produced by batch synthesis. They have an average diameter of  $193 \pm 25$  nm.

## Ceramics

Ceramics, such as silica and titania, are inorganic materials known best for their tolerance to high temperatures and corrosion. Ceramics are harder, stiffer, considerably less dense, and more resistant to deformation than similarly heat resistant metals, making them well suited for many high temperature applications particularly when weight is an issue. They also have low coefficients of thermal expansion which indicates that they undergo only minimal fluctuations in size in response to temperature changes. Ceramics are, however, very brittle and for this reason, when a metal would only dent a ceramic would completely shatter.<sup>32</sup>

### *2.1.2 Sol-Gel Chemistry*

Ceramics can be synthesized via sol-gel chemistry, which is a versatile process that can produce a variety of different materials including various colloids, ceramics, and glass, depending on the degree to and conditions under which processing is carried out.<sup>34, 35, 37</sup> The process involves the hydrolysis and subsequent condensation of a specifically selected precursor to produce a colloidal suspension of uniformly distributed nano- or micro- scale particles.<sup>29, 30, 31, 32</sup> The suspension can become a gel under the appropriate reaction conditions and if the reaction is allowed to continue until it reaches the gel point. The gel point is the time at which the last bond forms to complete a continuous solid skeleton that encloses the liquid phase.<sup>29, 34</sup>

The gel can be processed to produce a specific type of gel, such as an aerogel or a hydrogel, or it can undergo sintering or other extreme temperature treatments to produce a ceramic.<sup>31</sup> The key in processing different sol-gels depends primarily on the way in which solvents are removed from the gel. In the case of aerogels, the solvent is removed through the use of supercritical fluids and sublimation. This process ensures that the removal of the fluid does not cause interfacial forces to collapse the skeletal structure of the gel.<sup>35</sup> Figure 2.2 provides a representation of the sol-gel process and its versatility.

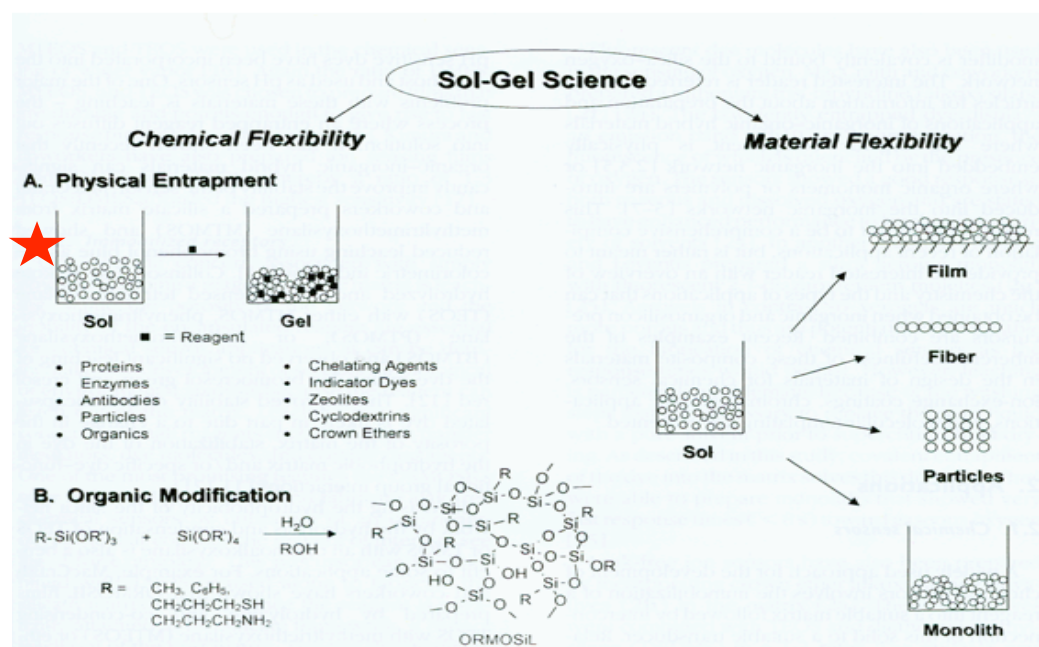


Figure 2.2. The sol-gel process is very versatile as it enables the formation of gels or sols, each of which can then be processed in various ways to get different products. In this project the goal is to produce sols so that the uniformly suspended particles can be isolated and analyzed.

Of specific interest in this case is the suspension of particles—a sol—which contains nano or micro scale ceramic spheres. A sol is a form of a colloid in which solid particles are dispersed in a liquid. If the process was allowed to proceed to the gel phase, the product would be useless for the purposes of this study because the particles would no longer be discrete.

The solid particles, which are denser than the liquid, must be small enough for gravitational forces to be negligible and for dispersion and van der Waals forces to be dominant. If the particles are large enough for gravitational forces to take hold they will settle on the bottom of the reaction vial and will not form a proper gel. Further, the particles must not be so small that they can be considered molecules in solution.<sup>29, 31</sup> These constraints require that the particles be submicron in diameter, in the range of two to several hundred nanometers.<sup>29, 31</sup> The inertia of the dispersed particles is small enough so that their movement is governed by Brownian motion through collisions with solvent molecules.<sup>29</sup>

### *2.1.3 History of Sol-Gel Chemistry*

Ebelmen and Graham are credited with discovering sol-gel science with their study of silica gels in the mid-nineteenth century.<sup>31, 34, 35</sup> They discovered that the acid catalyzed hydrolysis of tetraethoxysilane (TEOS) produced silicon dioxide in a viscous, glassy form, from which fibers could be drawn or composites formed. Their work with this reaction did not extend much farther

because drying this product to make a gel took a year in order to avoid cracking and fracture, and since their focus was on gels this method did not seem useful.<sup>35</sup>

Interest in sol-gel chemistry waned in and out over the next century, temporarily piquing the interest of various chemists along the way.<sup>29, 35</sup> The 1950's and 1960's saw a swell in the research involving colloidal silica particles in various fields including, catalysis, glass processing, ceramics, and nuclear fuel.<sup>29, 31, 35</sup> Roy et al turned to colloidal silica gels to make ceramics with greater chemical homogeneity than was possible with traditional ceramic powder methods, and Kolbe successfully synthesized uniform silica particles.<sup>39</sup> Iler studied silica chemistry and laid the foundation for later studies of the sol gel synthesis of silica as well as the commercial production of colloidal silica powders. Stober continued with Iler's work and developed a method to produce suspensions of monodisperse silica particles.<sup>35</sup>

In 1968 Werner Stober published a paper titled "Controlled Growth of Monodisperse Silica Spheres in the Micron Size Range" in the Journal of Colloid and Interface Science which outlines his process for producing suspensions of uniform silica spheres. It also details the influence that changing various reaction conditions has on the reaction rate, physical properties, and size distributions of the particles produced.<sup>39</sup> Stober's conclusions were, and remain today, of great importance to the field of sol-gel science and particularly the synthesis of monodisperse silica microspheres.<sup>35</sup> Stober's method of producing microsphere



suspensions is referred to as the Stober process and is currently used by many research groups.<sup>5, 35, 37</sup>

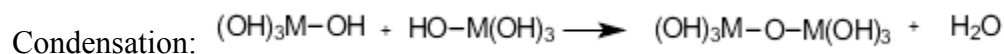
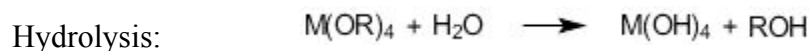
Prior to Stober's paper, successful attempts to synthesize monodisperse suspensions of silica particles were few. About a decade before Stober's work was published Kolbe, in 1956, produced silica particles by reacting tetraethyl silicate with water in an alcoholic solvent under basic conditions. Uniform silica spheres formed, but did so very slowly and required very pure reagents. Stober began his work here and developed a method to produce uniform silica suspensions that was faster and more tolerant to impurities than Kolbe's method.<sup>39</sup>

#### 2.1.4 *The Process*

The Stober process, and the sol-gel method in general, always begins with the selection of the precursors. There are several types of precursors available to chemists to carry out sol-gel reactions, although metal alkoxides are, by far, the most popular choice for the synthesis of inorganic materials.<sup>30, 37</sup> A precursor must be highly soluble in organic solvents, easily hydrolyzed, stable in solution, and easily purified. Metal alkoxides meet all of these criteria.<sup>30</sup>

Metal alkoxides consist of a metal or metalloid atom bound to alkoxy ligands that are usually aliphatic.<sup>29, 32, 34</sup> They are produced by reacting solid metal with the alcohol of the desired ligand. The metal alkoxide of most metals can be formed, although the reaction is not always a straightforward and simple one as several different products may be formed at once.

The mechanisms of hydrolysis and condensation differ slightly between silica and titania, mainly because the central atom of the former is a metalloid and that of the latter is a metal.<sup>36</sup> In general, however, both undergo hydrolysis and condensation as follows:<sup>29, 35</sup>



The sol-gel processing route to ceramic synthesis has many advantages over traditional methods; the low reaction temperature makes for safer and simpler execution and reduces the interactions between the ceramic and the reaction vessel wall. Further, the low reaction temperature, along with the dilute concentrations of reactants used in this process, allows for greater control over reaction kinetics. Pure final products are easier to achieve by simply purifying the precursor compounds by crystallization or distillation, for example, and dust contamination is minimized because the solid particles are in a liquid medium.<sup>31</sup>

### 2.1.5 *Synthesis of Silica Microspheres*

Tetraethoxysilane (TEOS) is the precursor used for silica synthesis, as shown in Figure 2.3. The central atom of the molecule is silicon, which is a weak Lewis acid and is not particularly electrophilic.<sup>36</sup> The partial positive charge on the silicon atom is only +0.32 which is low compared to that of metals such as titanium and zirconium in their respective ethoxides, which are +0.63 and +0.65 respectively.<sup>29</sup> The mediocre partial positive charge on silicon does not make it

particularly susceptible to nucleophilic attack which is necessary for its hydrolysis. For hydrolysis to occur on a silicon alkoxide the reaction must, therefore, be catalyzed.<sup>36</sup>

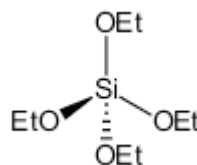


Figure 2.3. Tetraethoxysilane (TEOS) is the precursor used for silica synthesis.

The reaction can be catalyzed by either an acid or a base. In the presence of a basic catalyst, the reaction follows an  $S_N2$  mechanism as shown in Figure 2.4.

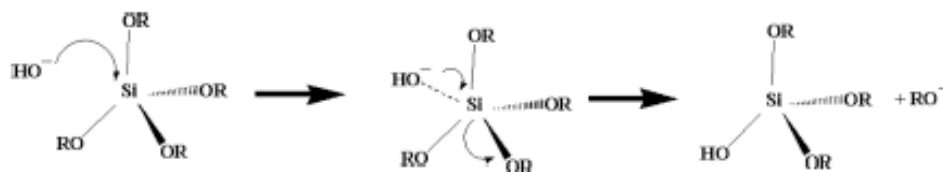


Figure 2.4.<sup>36</sup> The mechanism for the base catalyzed hydrolysis of a silicon alkoxide.

A hydroxide ion, which is a very strong nucleophile, attacks the silicon atom because it carries the most positive charge in the molecule, and causes the formation of a pentavalent transition state. One of the OR groups is then removed as an  $RO^-$  ion, because it is a better leaving group than  $HO^-$  due to its slightly

lower nucleophilicity.  $\text{RO}^-$  then reacts with  $\text{H}_2\text{O}$  to regenerate the hydroxide catalyst.<sup>35, 36</sup> The silicon alkoxide can be partially hydrolyzed, as shown in Figure 2.4, or completely hydrolyzed, in which all OR groups are replaced by OH groups.<sup>31, 35</sup>

The acid catalyzed hydrolysis proceeds by a different mechanism than the base catalyzed reaction, as shown in Figure 2.5.

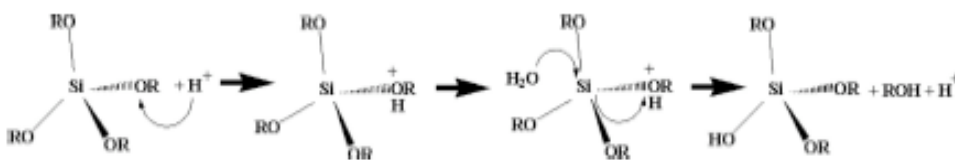


Figure 2.5<sup>36</sup> The mechanism for the acid catalyzed hydrolysis of a silicon alkoxide.

In this case a hydrogen ion catalyst binds with the oxygen on one of the ligands of the silicon alkoxide, generating a positive charge and shifting the electron density towards the ligand. This shift increases the partial positive charge on the silicon, making it more susceptible to nucleophilic attack. Water attacks the silicon atom and facilitates the removal of ROH, which is a good leaving group because leaving relieves the oxygen atom of the positive charge. This reaction occurs faster than the based catalyzed reaction because in this case the silicon atom serves as a Lewis base, or an electron donator, which it does much more easily than serving as a Lewis acid.<sup>35, 36</sup>

Condensation reactions occur simultaneously to hydrolysis.<sup>29, 35</sup> For this reason and because there may be several condensation reactions occurring at once, it is difficult to determine the mechanisms and kinetics for condensation with certainty. Nevertheless, partially or fully hydrolyzed silicon alkoxide molecules condense to form siloxane bonds, or Si-O-Si linkages, eliminating a water or alcohol molecule in the process. As more linkages are created, more molecules are connected and a particle begins to form.<sup>35</sup> The initially formed particles serve as nuclei for continued growth by Ostwald Ripening in which small and highly soluble particles precipitate on these nuclei to form larger particles.<sup>29</sup>

The reaction conditions, including concentrations and natures of reactants, pH, temperature, and type of solvent, all contribute to the quality of the silica particles produced.<sup>35, 39</sup> Most of the conclusions about how reaction conditions affect particle formation have been made based on qualitative observations rather than quantitative ones because of the complexities and overlapping of reactions in the sol-gel process.<sup>35</sup>

Despite the faster reaction rate under acidic conditions, there are several reasons why base catalysis is more suitable when sols, as opposed to gels, are the desired end product.<sup>5, 29, 39</sup> Base catalyzed silica synthesis, called the Stober Process, has been shown to increase the rate of condensation, which may favor the formation of compact particles over extended networks and, therefore, more easily produce a uniformly distributed suspension rather than a gel. The

formation of a sol is desirable because the particles can be isolated and studied. Additionally, Si NMR studies have shown that condensation products are generated in the sequence of monomer, dimer, linear trimer, cyclic trimer, cyclic tetramer, and then higher order molecules that become particles. Ring opening of the cyclic species is necessary for continued growth, but the rate of ring opening in an alcohol is very low at an acidic pH because silica is insoluble under these conditions. The insolubility prevents rearrangement into particles and the formation of an extended network that becomes a gel supersedes the formation of a sol.<sup>29, 35</sup>

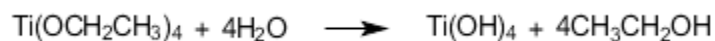
Ammonia is a common reagent to use as a basic catalyst, and Stober demonstrated that the spherical morphology of silica particles is heavily dependent on its presence; the particles lost their shape in its absence. He also showed that increasing the concentration of ammonia increases the size of the silica particles, concluding that a reaction solution saturated with ammonia gives the largest particles. For the formation of silica spheres in an ethanol solvent with a tetraethoxysilane (TEOS) precursor, the largest particles that can be formed have a diameter of 1  $\mu\text{m}$ , according to Stober.<sup>39</sup>

The concentration of TEOS contributes to the morphology of the particles as well. If the concentration of this precursor exceeds 0.2 M the particles begin to lose their spherical shape and become more polydisperse.<sup>29</sup> Stober, however, reports that the concentration can be increased to 0.5 M without significant effects on the quality and size distribution of the particles.<sup>35</sup>

### 2.1.6 Synthesis of Titania Microspheres

The specifics of the silica model cannot be directly applied to titania because silicon is a metalloid and titanium is a metal and they exhibit different reactivities. Nevertheless, the process still begins with a metal alkoxide precursor. Similar to the synthesis of silica, a titanium alkoxide precursor undergoes hydrolysis and condensation, however, the hydrolysis reaction does not need to be catalyzed in this case. Catalysis is unnecessary because titanium is a strong Lewis base and much more reactive than silicon.<sup>36</sup> Again, the partial positive charge on titanium is about +0.63 when bound to ethoxy ligands, while it is only +0.32 for silicon with the same ligands.<sup>29</sup> A titanium alkoxide reacts with water to undergo uncatalyzed hydrolysis  $10^5$  to  $10^8$  times faster than does a silicon alkoxide.<sup>36</sup> Even though acid/base catalysis is unnecessary, a neutral pH is still undesirable because it eliminates the presence of a surface charge on the particles which can lead to aggregation in the absence of electrostatic repulsion between particles.<sup>41</sup> Titanium alkoxide's reactivity also means that the titanium alkoxide precursor is particularly susceptible to moisture in the air and attention must be paid to the reaction, storage, and handling environments.<sup>29</sup>

In 1985 Barringer and Bowen synthesized sols of uniform  $\text{TiO}_2$  particles by hydrolyzing titanium tetraethoxide in ethanol. They concluded that hydrolysis occurred in ethanol via the following reaction. This particular scheme represents complete hydrolysis, although partial hydrolysis can also occur.



Condensation follows, in which the hydrolysis products polymerize to form networks of Ti-O-Ti bonds that grow into nuclei and eventually particles.

Hsu and Nacu produced a study in 2003 that investigated the impact that a selection of reaction variables, such as pH, temperature, and reactant concentrations, had on the synthesis of uniform titania sols. They performed their reaction under acidic conditions, established by the addition of hydrochloric acid to the reaction vessel, and used titanium isopropoxide as their precursor. They observed that the acid concentration and the water/alkoxide ratio were the most influential parameters on the size and size distribution of the particles. Both the particle size and size distribution increased as the acid concentration or water/alkoxide ratio were increased. They also claimed that the presence of an acid is essential to forming a sol, as it catalyzes the reaction and prevents agglomeration by introducing electrostatic repulsions between the particles.<sup>41</sup> These findings were the basis of the titania synthesis recipe in this project, however, further investigation revealed that several other groups created a basic reaction environment and achieved better results, as will be discussed shortly.<sup>35, 40</sup>

In this project, the batch reactor, single phase microreactor, and segmented flow microreactor constructed in Chapter 1 were used for the synthesis of silica and titania microspheres by the sol-gel process. The goal was to produce microspheres with a narrow size distribution and to do so with a method that achieved reproducible results. It was expected that the segmented flow



microreactor would produce microspheres with the narrowest size distribution, followed by the batch reactor, and finally the single phase microreactor. The segmented flow microreactor was expected to perform the best because the reaction took place within nano-beakers. The results in Chapter 1 show that the periodicity of the nano-beakers is reproducible and, therefore, that the segmented flow microreactor offers precise control over the reaction time. The nano-beakers also exhibit minimal dispersion and enhanced mixing, as discussed in Chapter 1, which was expected to improve the size distribution of the particles compared to those produced in a single phase microreactor.

## 2.2 Experimental Methods—Synthesis of Ceramic Microspheres

### 2.2.1 *Materials for the Synthesis of Silica*

Ammonium hydroxide, methanol, and 95% ethanol, all purchased from Sigma, and tetraethoxysilane 99+% (Gelest, Morrisville, PA) were used as provided. Nanopure water was collected from a MilliQ system.

### 2.2.2 *Characterization of Batch Synthesis of Silica*

Batch synthesis of silica microspheres was carried out by the Stober process with a modified version of the recipe outlined by Khan, et al.<sup>5</sup> A solution of 13.0 M H<sub>2</sub>O and 1.0 M NH<sub>3</sub> in ethanol was combined in a 1:1 volumetric ratio with 0.1 M tetraethoxysilane in ethanol. The solution was mixed using a magnetic stir bar and stirrer for reaction times of 5, 10, 15, and 20 minutes. After about ten minutes the solution began to turn increasingly more opaque and turbid. The resulting solutions were diluted in 1:10 volumetric ratio with methanol and analyzed with a DLS (Malvern Instruments, Zetasizer Nano-S, Worcestershire, UK) to measure microsphere diameter. One drop of the diluted solution for each residence time was spin coated at 1500 rpm onto a silica wafer cleaned with ethanol. The wafers were then sputter coated with a layer of gold approximately 5 nm thick and imaged under an SEM (Quanta, Hillsboro, OR). The microspheres were examined under a vacuum pressure of about 10<sup>-6</sup> torr and with

an accelerating voltage of 20.0 kV. The spot size was 2.5. The diameters of 100 microspheres for each residence time were measured from the SEM images using Image J to determine the average microsphere diameter for each sample.

### *2.2.3 Characterization of Single Phase and Segmented Flow Synthesis of Silica*

Silica microspheres were synthesized in the single phase microreactor shown in Figure 1.18. The same recipe was used for laminar flow synthesis as was used for the batch synthesis of silica: a solution of 13.0 M H<sub>2</sub>O and 1.0 M NH<sub>3</sub> in ethanol was loaded in one syringe and a solution of 0.1 M TEOS in ethanol was loaded in the second and they were injected into the microreactor at identical flow rates, mimicking the 1:1 volumetric ratio of reagent solutions used in batch synthesis. The length required of the aging capillary was calculated to allow for the collection of samples with residence times of 5, 10, 15, and 20 minutes while employing flow rates between 2 uL/min and 20 uL/min for each syringe. The volume of the aging capillary was determined by calculating the volume of a cylinder with a diameter equal to the inner diameter and a height equal to the length of the capillary. Specific flow rates were then calculated to produce the desired residence times. It was assumed that the flow rate indicated by the syringe pumps was the true flow rate.

Single phase flow synthesis of silica was characterized in a microreactor with a 150  $\mu\text{m}$  inner diameter (ID) aging capillary and with a 250  $\mu\text{m}$  ID aging

capillary, while always keeping the inner diameter of all remaining capillary 150  $\mu\text{m}$ . Table 2.1 shows the residence times and their corresponding flow rates and aging capillary dimensions.

Table 2.1. Details of microreactor settings for each residence time for the single phase microreactor.

<b>Residence Time (min)</b>	<b>Flow Rate TEOS (<math>\mu\text{L}/\text{min}</math>)</b>	<b>Flow Rate <math>\text{H}_2\text{O}/\text{NH}_3</math> (<math>\mu\text{L}/\text{min}</math>)</b>	<b>Length of Aging Capillary (m)</b>	<b>Aging Capillary Diameter (<math>\mu\text{m}</math>)</b>
5	10.6	10.6	6	150
10	5	5	6	150
15	3.53	3.53	6	150
20	2.65	2.65	6	150
25	2.12	2.12	6	150
5	10.6	10.6	2.1	250
10	5	5	2.1	250
15	3.53	3.53	2.1	250
20	2.65	2.65	2.1	250

For every residence time, the system was allowed to run for 20 to 30 minutes plus the length of the residence time at the desired flow rates before timing began to allow for equilibration of the syringe pumps. After the total equilibration period and residence time had elapsed, two samples were collected back to back by placing the end of the aging capillary in an Eppendorf tube filled with about 700 to 800  $\mu\text{L}$  of methanol. The exact volume of methanol required as well as the duration of the collection period were calculated to produce a 1:10 volumetric ratio of product to solvent based on the total flow rate in the aging

capillary. After collection of the samples, ten drops of each were spin coated at 1500 rpm for one minute onto separate silica wafers cleaned with ethanol. Each sample was also further diluted and then analyzed with the DLS.

The method of collecting product from the microreactor was developed after trying many different techniques. These included scanning the end of the capillary across a cleaned silica wafer, allowing the ethanol to evaporate on its own, as well as holding the end of the capillary steady on a silica wafer while wicking away ethanol with a Kimwipe in hopes that the microspheres would remain deposited on the substrate. The results of each attempt were imaged on the SEM and revealed agglomerations of indiscrete material. Collection in methanol, followed by spin coating ten drops of this solution on a silica wafer produced much better images that showed clearly defined spheres.

The silica-mounted samples were sputter coated with a layer of gold approximately 5 nm thick and were examined under an SEM with the same conditions used for the batch synthesis samples. The diameters of 100 microspheres, or as many as possible if there were not 100 distinct spheres, were measured from the SEM images with Image J. After the samples for all desired residence times were collected the system was flushed with ethanol to wash out all reagents and prevent the development of any clogs due to gelation of silica.

Segmented flow synthesis of silica was performed under the same basic conditions as synthesis in the single phase microreactor with a few modifications. The apparatus was set up as depicted in Figure 1.19, with the gas flowing into a

segmenting T-junction where it met with the reagent stream. The residence times and corresponding flow rates are shown in Table 2.2 along with the length of the aging capillary which had to be adjusted due to the addition of the gas. A 4.3 m piece of 250  $\mu\text{m}$  ID aging capillary was used. No trials were performed with a 150  $\mu\text{m}$  ID aging capillary because the 250  $\mu\text{m}$  aging capillary produced microspheres with a more distinct morphology than the former in the single phase microreactor. The equilibration time for each residence time varied, as the volume of the gas syringe was considerably lower than that of the reagent syringes and could run for a much shorter time. The equilibration times ranged from about 10 minutes for the 5 minute residence time samples to about 45 minutes for the 20 minute residence time samples.

After equilibrating, the microreactor was allowed to run for the duration of the residence time before collecting began. The samples were collected and analyzed with the SEM and DLS with the same procedure used in the single phase flow experiments.

Table 2.2. Flow rates of reagents and gas for each residence time in the segmented flow microreactor.

<b>Residence Time (min)</b>	<b>Flow Rate TEOS (<math>\mu\text{L}/\text{min}</math>)</b>	<b>Flow Rate <math>\text{H}_2\text{O}/\text{NH}_3</math> (<math>\mu\text{L}/\text{min}</math>)</b>	<b>Flow Rate Gas (<math>\mu\text{L}/\text{min}</math>)</b>
5	10.6	10.6	21.2
10.6	5.00	5.00	10.0
15	3.53	3.53	7.06
20	2.65	2.65	5.30

#### 2.2.4 *Materials for the Synthesis of Titania*

2-propanol, and glacial acetic acid (17.4M), purchased from Sigma, and titanium isopropoxide (Gelest, Morrisville, PA) were used as provided. Nanopure water was collected from a MilliQ system.

#### 2.2.5 *Characterization of Batch Synthesis of Titania*

Batch synthesis of titania microspheres was carried out using a procedure similar to that by which the silica microspheres were produced. The recipe outlined by Hsu, et al<sup>41</sup> was manipulated until well formed microspheres exhibiting minimal aggregation were formed. The best results were achieved when a solution of 0.17 M  $\text{H}_2\text{O}$  and 3.41 M glacial acetic acid ( $\text{CH}_3\text{COOH}$ ) in 2-propanol was mixed in a 1:1 volumetric ratio with a solution of 0.1 M titanium

isopropoxide in 2-propanol. The titanium isopropoxide solution was made in a scintillation vial in order to minimize the reagent's exposure to and reaction with moisture from the air. As an additional precaution, all vials containing titanium isopropoxide were sealed with parafilm when not in use. The  $\text{H}_2\text{O}/\text{CH}_3\text{COOH}$  solution was added to the vial containing the titanium isopropoxide and mixed on a magnetic mixer with a stir bar for 2.5 hours. The solution was then allowed to sit with no mixing for another 1.5 hours before analyzing the sample with the DLS. Since the solution remained clear even after 4 hours it was not diluted. One drop of the solution was spin coated at 1500 rpm for one minute on a silica wafer cleaned with 2-propanol. The wafer was then sputter coated with gold for 30 seconds to give a coating of approximately 5 nm, and the sample was examined with an SEM under the same conditions as used for the SEM analysis of the batch synthesis of silica. The average diameter of 100 microspheres was calculated by measuring the microsphere diameter with Image J.

### *2.2.6 Characterization of Single Phase Flow Synthesis of Titania*

Titania microspheres were synthesized in the laminar flow microreactor using the same recipe as used for batch synthesis of titania. The microreactor was set up according to Figure 1.18. One syringe was loaded with a solution of 0.1 M titanium isopropoxide,  $\text{Ti}(\text{OPr})_4$ , in 2-propanol, and the other syringe was loaded with a solution of 0.17 M  $\text{H}_2\text{O}$  and 3.41 M acetic acid in 2-propanol. The flow



rates of the two reagent solutions were identical to keep the reagents in a 1:1 volumetric ratio. The residence times used for this reaction were 15 minutes, 30 minutes, and 60 minutes. These residence times were less than the reaction time used in batch synthesis. This was done for practical reasons as well as because the results of silica synthesis in the laminar flow microreactor show that the microspheres grow faster in the microreactor than they do in the batch reactor. The aging capillary had an inner diameter of 250  $\mu\text{m}$  and a length of 9 m, which was calculated to achieve the desired residence times while using flow rates between 2  $\mu\text{L}/\text{min}$  and 20  $\mu\text{L}/\text{min}$  for each reagent solution. Table 2.3 shows the residence times and the corresponding flow rates.

Table 2.3. Microreactor settings for each residence time for titania synthesis in the single phase microreactor.

<b>Residence Time (min)</b>	<b>Flow Rate Ti(OPr)<sub>4</sub> (<math>\mu\text{L}/\text{min}</math>)</b>	<b>Flow Rate H<sub>2</sub>O/CH<sub>3</sub>COOH (<math>\mu\text{L}/\text{min}</math>)</b>
15	14.7	14.7
30	7.30	7.30
60	3.68	3.68

For each residence time, the microreactor was allowed to equilibrate for 30 minutes before timing the residence time. Two samples for each residence time were collected back to back in Eppendorf tubes containing about 800  $\mu\text{L}$  of 2-propanol. The exact volume of 2-propanol and the duration of the collection period were calculated to produce a 1:10 ratio of product to solvent based on the

total flow rate in the aging capillary. The samples were analyzed with the SEM and DLS in the same way that the microreactor-produced silica samples were analyzed with one difference: 2-propanol was used in place of methanol and ethanol. After the samples for all of the residence times had been collected the microreactor was flushed with 2-propanol to remove remaining reagents and minimize clogging.

## 2.3 RESULTS AND DISCUSSION

In the following data there are discrepancies between the SEM and DLS values. The SEM data is the more reliable of the two, for several reasons, and will be considered in higher regard than the DLS data. In analyzing a sample with the DLS, any aggregation will introduce error in the measurements as an aggregate will be seen as a large particle by the instrument. Aggregation, therefore, may cause the reported average diameter to be greater than the true average diameter, and it will increase the size distribution measurements. The DLS reports the hydrodynamic diameter of the particles and this measurement can be influenced by the presence of ions in the sample, usually reporting a diameter that is greater than the true value.<sup>55</sup> The SEM is also subject to error in the form of hysteresis, which can render the scale bar inaccurate to about 10 nm. These measurements, however, were made using a standard diffraction grating with known dimensions to set the scale with which to measure the microspheres. Although this method is time consuming, it eliminates the problem introduced by hysteresis and produces more accurate results.

### 2.3.1 *Batch Synthesis of Silica*

Figure 2.6 shows the average diameters of the microspheres produced in the batch reactor as determined from analysis of SEM images. DLS data is not available for this reactor.

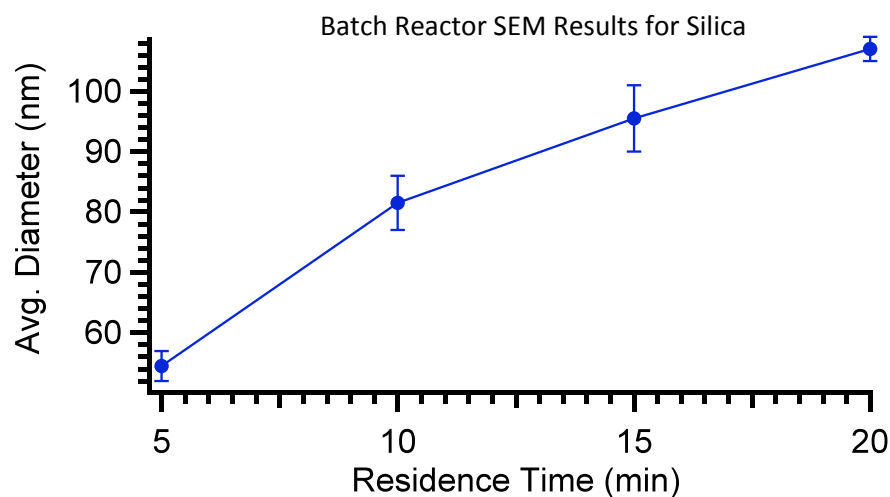


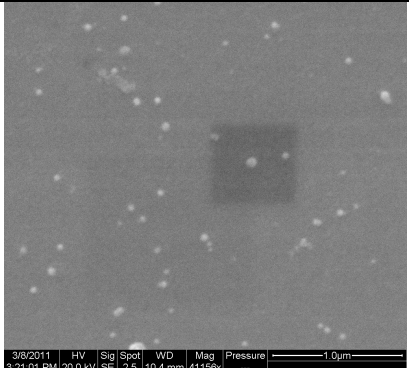
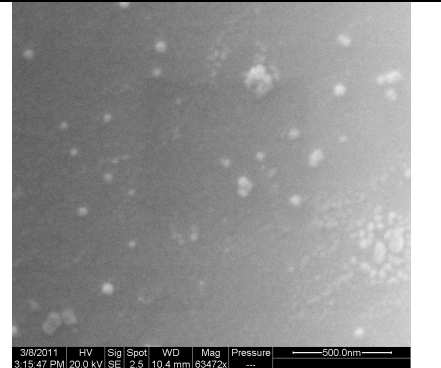
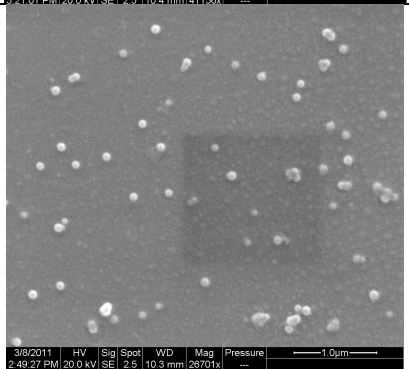
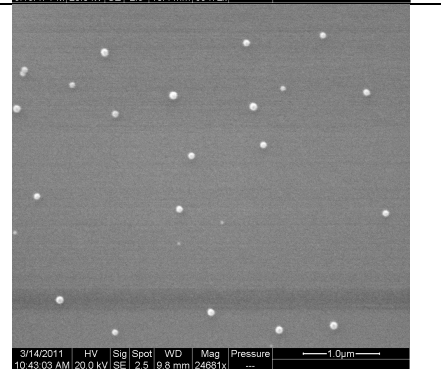
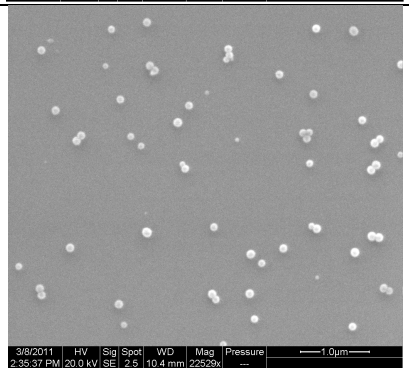
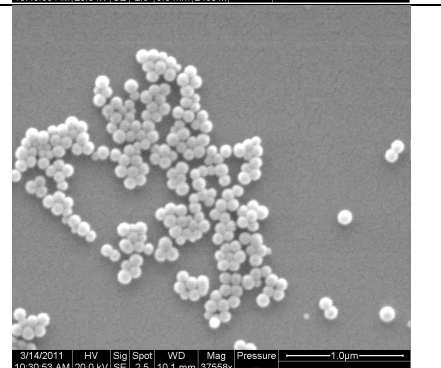
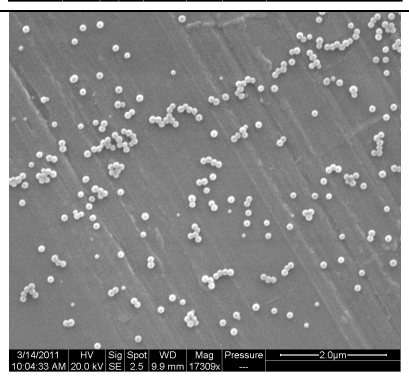
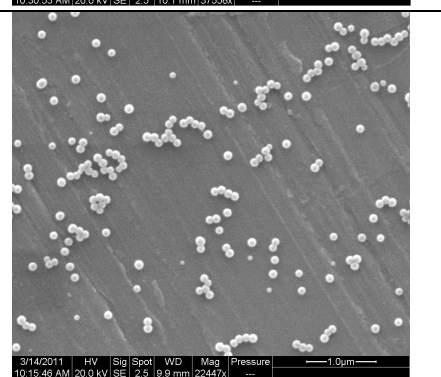
Figure 2.6. The average diameter of silica microspheres produced by batch synthesis as determined from SEM images.

The microsphere diameters range from  $54.5 \pm 2.5$  nm ( $n = 2$ , 4.58% RSD) to  $107 \pm 2.0$  nm ( $n = 2$ , 1.87% RSD) and they increase as the residence time increases, as expected due to the fact that the particles have a longer growth period with longer reaction times. The longer the reaction time, the greater the average diameter of the particles as a result of the longer growth periods that accompany longer reaction times. The rate of growth slows as the reaction time increases, implying that microspheres with lower residence times are particularly sensitive to the reaction time.

The 10 and 15 minute samples show the widest size distribution; the average diameter of the 10 minute sample is  $81.5 \pm 4.5$  ( $n = 2$ , 5.52% RSD) and the 15 minute sample  $95.5 \pm 5.5$  ( $n = 2$ , 5.76% RSD). The size distributions are

low for all residence times, never exceeding 5.76% deviation. The images in Table 2.4 are all from the samples of the same batch, corresponding to the values displayed in Figure 2.6. The spheres are well formed and of a narrow size distribution

Table 2.4. SEM images of silica microspheres produced in the batch reactor for each of the residence times tested.

Residence Time (min)	Batch Synthesis	
5	 <p>3/8/2011 HV Sig Spot WD Mag Pressure 3:21:01 PM 20.0 kV SE 2.5 10.4 mm 41158x ...</p>	 <p>3/8/2011 HV Sig Spot WD Mag Pressure 3:15:47 PM 20.0 kV SE 2.5 10.4 mm 63472x ...</p>
10	 <p>3/8/2011 HV Sig Spot WD Mag Pressure 2:49:27 PM 20.0 kV SE 2.5 10.5 mm 23701x ...</p>	 <p>3/14/2011 HV Sig Spot WD Mag Pressure 10:43:03 AM 20.0 kV SE 2.5 9.8 mm 24681x ...</p>
15	 <p>3/8/2011 HV Sig Spot WD Mag Pressure 2:35:37 PM 20.0 kV SE 2.5 10.4 mm 22929x ...</p>	 <p>3/14/2011 HV Sig Spot WD Mag Pressure 10:30:53 AM 20.0 kV SE 2.5 10.1 mm 37558x ...</p>
20	 <p>3/14/2011 HV Sig Spot WD Mag Pressure 10:04:33 AM 20.0 kV SE 2.5 9.9 mm 17309x ...</p>	 <p>3/14/2011 HV Sig Spot WD Mag Pressure 10:15:46 AM 20.0 kV SE 2.5 9.9 mm 22447x ...</p>

Although this data represents a narrow size distribution, it does not speak to the reproducibility of microspheres between separate batches. For instance, silica was synthesized in the batch reactor on several different days with only a 20 minute residence time. The average diameter of microspheres from separate batches was determined from SEM images and their values are given in Table 2.5. As is evidenced by the disparity in these values, the batch reactor suffers from a lack of reproducibility and wide size variation between batches which warrants the development of a better synthesis device for these microspheres, such as a microreactor.

Table 2.5. Results for 20 minute residence time samples from different batches

	<b>Average Diameter (nm)</b>	<b>Standard Deviation (nm)</b>	<b>%RSD</b>	<b>Replicates (N)</b>
Batch 1	211	36	17.1	1
Batch 2	193	25	12.9	2
Batch 3	107	2	1.87	2

### 2.3.2 *Single Phase Microreactor Synthesis of Silica*

Figures 2.7 and 2.8 show the SEM and DLS results, respectively, of the average diameter determination of silica microspheres produced in the single phase microreactor with an aging capillary with a 150  $\mu\text{m}$  inner diameter (ID). Both SEM and DLS results indicate an increase in the microsphere diameter with a corresponding increase in residence time, as expected due to the longer growth

period inherent in longer residence times. The SEM results for the average diameter of the 5 and 15 minute samples were inconclusive because no spheres were found when the samples were imaged. This could be due to a problem during the reaction or during the spin coating process. Figure 2.7 suggests that the microspheres produced after 5 minute residence times would have an average diameter of less than 80 nm. If they were much smaller than this the SEM may not have been able to resolve them, which would explain why none were found.

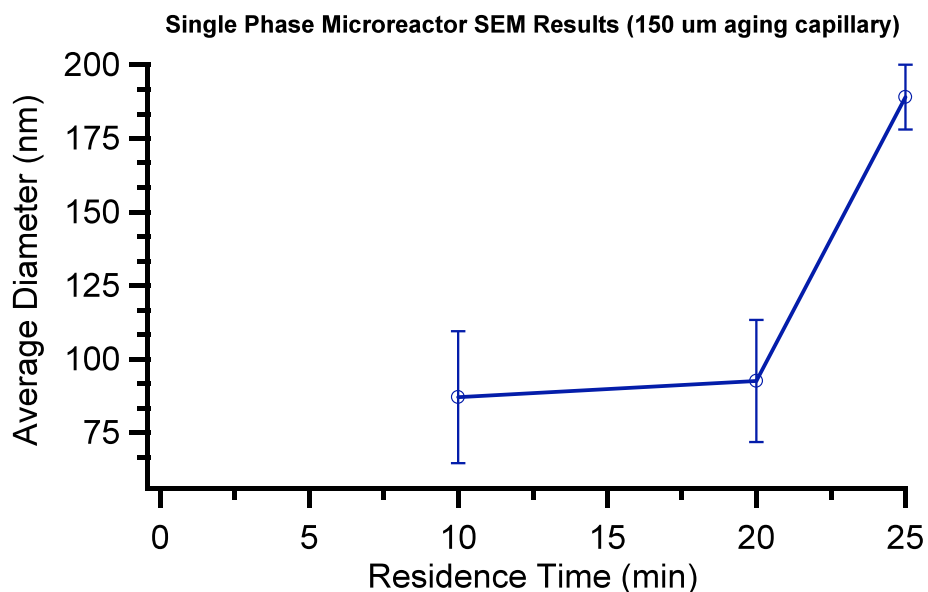


Figure 2.7. Average diameter of silica microspheres produced in the single phase microreactor with an aging capillary with an inner diameter of 150  $\mu\text{m}$ . This data was gathered from SEM images.



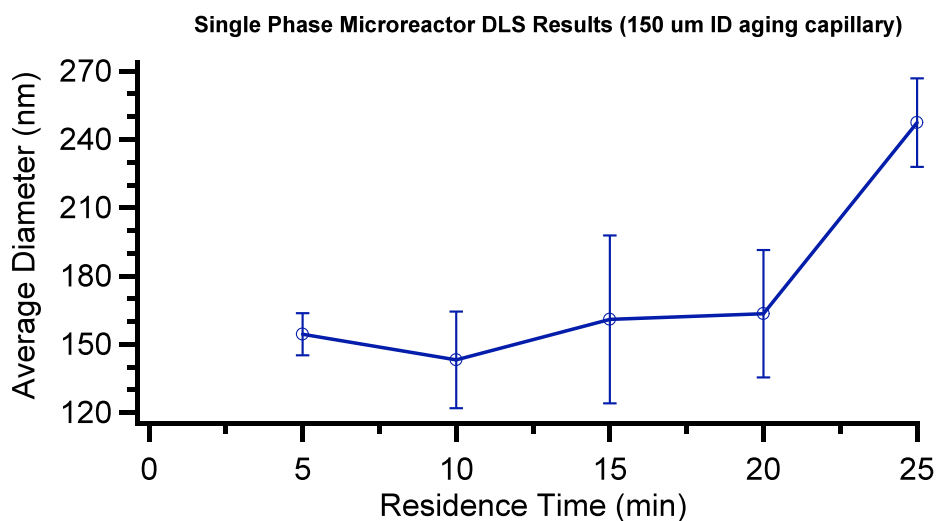


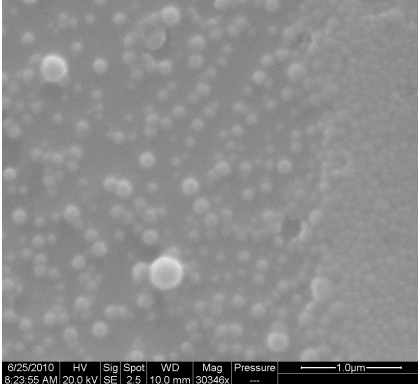
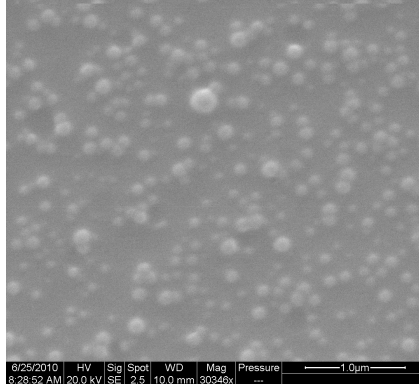
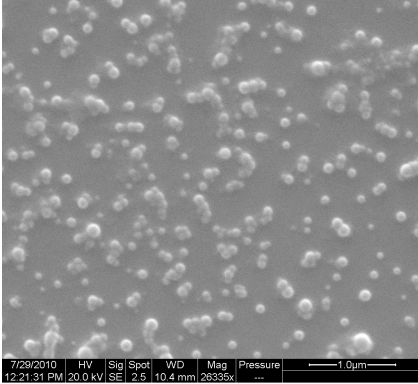
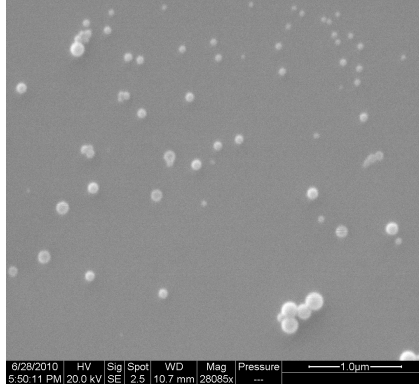
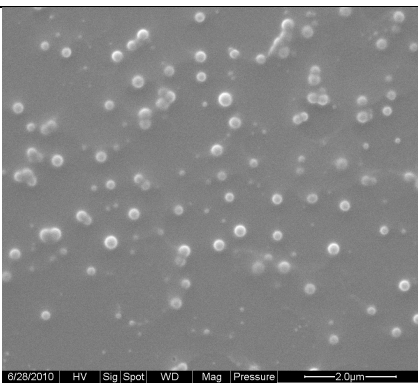
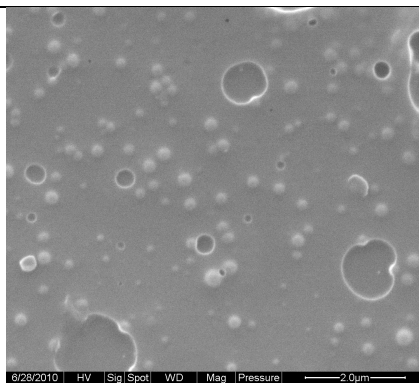
Figure 2.8. Average diameter of silica microspheres produced in the single phase microreactor with an aging capillary with an inner diameter of 150  $\mu\text{m}$ . This data was gathered from DLS measurements.

The average microsphere diameter for each residence time differs greatly between SEM and DLS data; the average diameter for a 5 minute residence time was determined to be  $154.4 \pm 9.2$  (n=2, 5.96% RSD) with DLS, while SEM results were inconclusive because no spheres were found. For the 10 minute residence time the DLS gave an average diameter of  $143.1 \pm 21.2$  nm (n=4, 14.8% RSD), and the SEM images gave a value of  $87.0 \pm 22.4$  nm (n=4 25.7% RSD). The 15 minute residence time samples had an average diameter of  $160.9 \pm 36.9$  nm (n=2, 22.9% RSD) according to the DLS and inconclusive SEM results. For the 20 minute residence time samples the DLS gave a value of  $163.4 \pm 28.0$  nm (n=4, 17.1% RSD) for the average microsphere diameter and the SEM gave a

value of  $92.5 \pm 20.7$  nm ( $n=4$ , 22.4% RSD). The 25 minute residence time samples had an average diameter of  $247.4 \pm 19.4$  nm ( $n=2$ , 7.84% RSD) according to the DLS and  $189 \pm 11$  ( $n=2$ , 5.6% RSD) according to the SEM results.

The size distributions produced by this microreactor are much larger than those produced by batch synthesis as indicated by the %RSD values and qualitatively by the SEM images in Table 2.6 which show a greater size variety for single phase flow microspheres than the batch microspheres. There is no obvious trend in the standard deviation or % RSD values for DLS data.

Table 2.6. SEM images of silica microspheres produced in the single phase microreactor with an aging capillary with an inner diameter of 150  $\mu\text{m}$ .

Residence Time (min)	Single Phase Microreactor (150 $\mu\text{m}$ ID aging capillary)	
5	<i>NO IMAGE</i>	
10		
15	<i>NO IMAGE</i>	
20		
25		

Silica synthesis was also carried out in a single phase microreactor with a 250  $\mu\text{m}$  ID aging capillary in an effort to improve the size distributions produced by the single phase device with a 150  $\mu\text{m}$  ID aging capillary. Improved size distributions were expected because the extent of dispersion decreases with an increase in the channel diameter.<sup>23</sup> The SEM and DLS results for these trials can be seen in Figures 2.9 and 2.10, respectively.

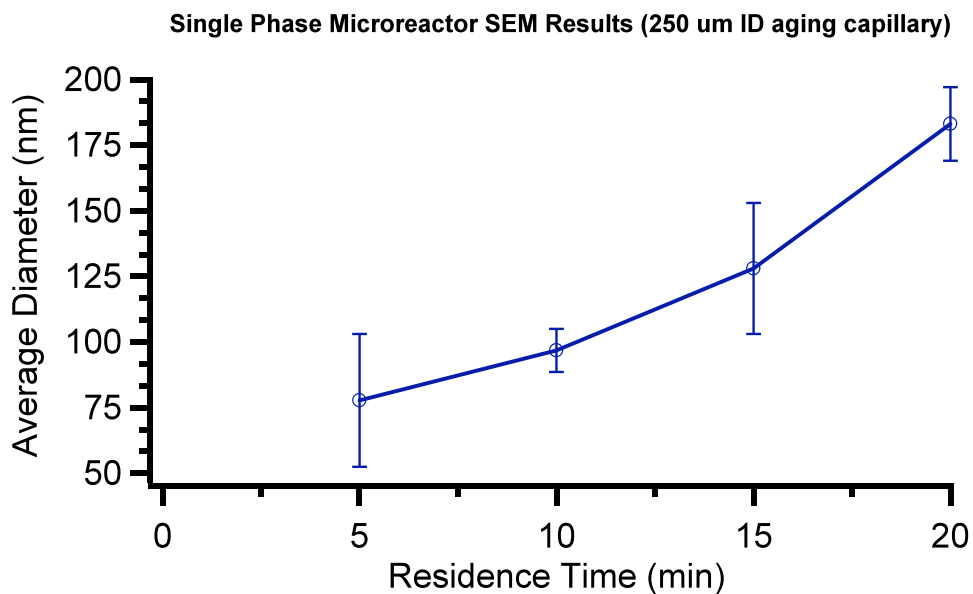


Figure 2.9. Average diameter of silica microspheres produced in the single phase microreactor with an aging capillary with an inner diameter of 250  $\mu\text{m}$ . This data was collected from SEM images.

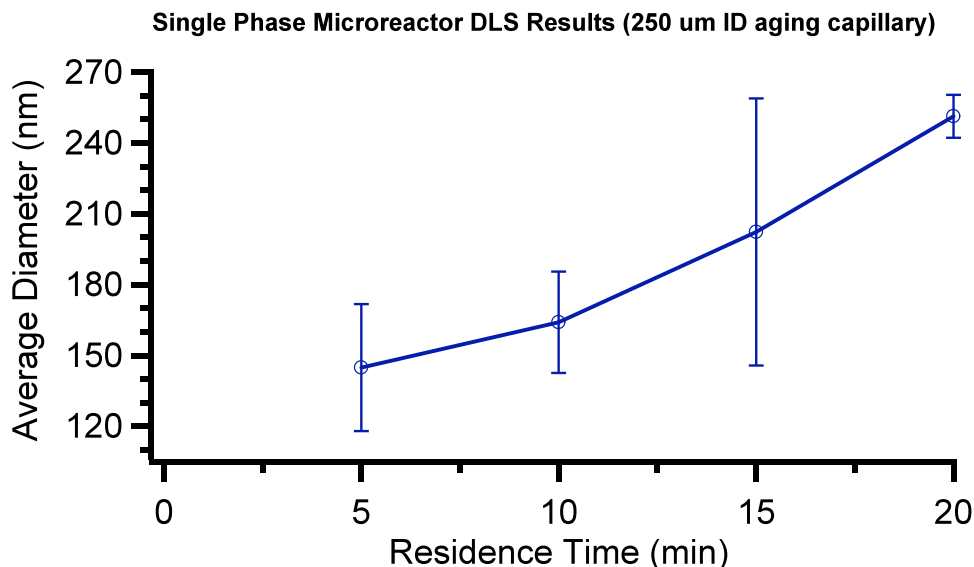


Figure 2.10. Average diameter of silica microspheres produced in the single phase microreactor with an aging capillary with an inner diameter of 250  $\mu\text{m}$ . This data was gathered from DLS measurements.

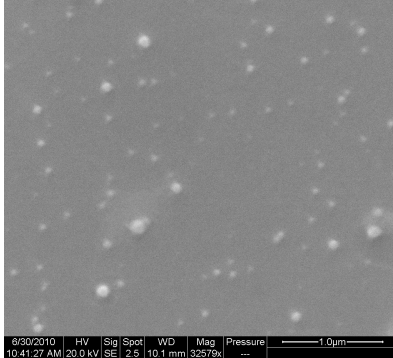
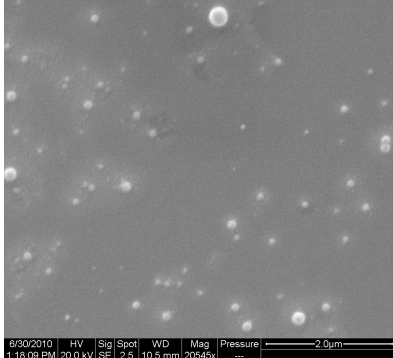
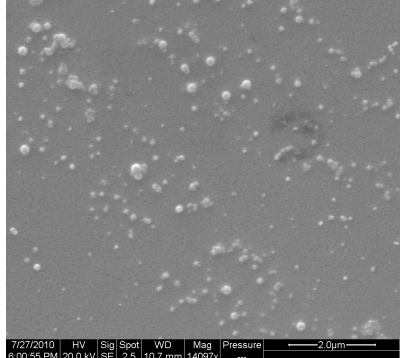
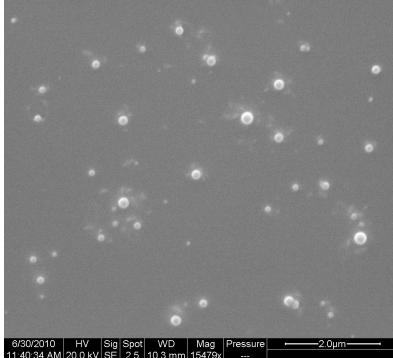
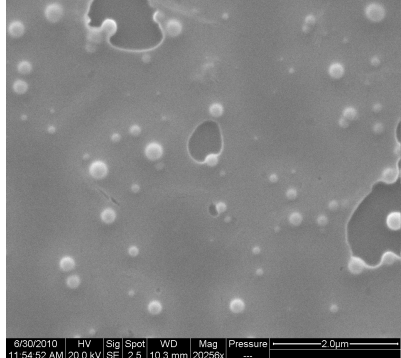
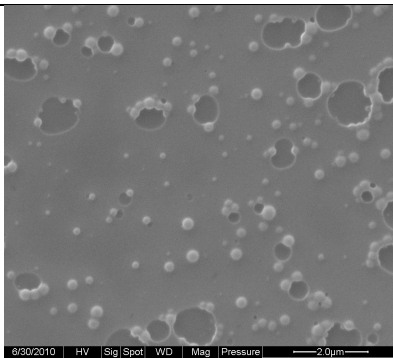
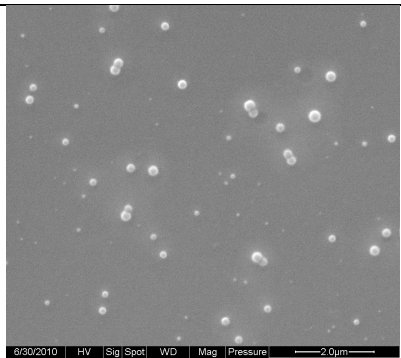
For the 5 minute residence time samples the DLS gives an average diameter of  $144.7 \pm 26.9$  nm ( $n=4$ , 18.6% RSD) and the SEM images give an average diameter of  $77.7 \pm 25.3$  nm ( $n=3$ , 32.6% RSD). The 10 minute residence time samples have an average diameter of  $164.0 \pm 21.5$  nm ( $n=4$ , 13.1% RSD) according to the DLS and  $96.7 \pm 8.2$  nm ( $n=3$ , 8.5% RSD) according to SEM results. For the 15 minute residence time samples the DLS gives an average diameter of  $202.3 \pm 56.6$  nm ( $n=4$ , 28.0% RSD) and the SEM results give an average diameter of  $128 \pm 25$  nm ( $n=3$ , 20% RSD). The 20 minute residence time samples have an average diameter of  $251.3 \pm 9.1$  nm ( $n=4$ , 3.6% RSD) according to the DLS and  $183 \pm 14$  nm ( $n=3$ , 7.9% RSD) according to SEM results.

The microspheres produced by this microreactor show an increase in average diameter as residence time increases, just as in the batch reactor and the single phase microreactor with a 150  $\mu\text{m}$  ID aging capillary. Comparison with the batch synthesis data shows that the rate of particle growth is faster in this microreactor than in the batch reactor, as the average diameter of the microspheres is greater for the microreactor than for the batch reactor for all of the residence times.

The size distributions produced by this microreactor are difficult to interpret due to the high standard deviation of 25.0 nm for the 15 minute residence time samples. Excluding this data point, the size distribution decreases as the residence time increases potentially as a result of reduced dispersion at the slower flow rates inherent in longer residence times.

Once again, the size distributions of these samples are greater than those of batch synthesis as shown by the %RSD values as well as the SEM images in Table 2.7. These results are in agreement with our expectations.

Table 2.7. SEM images of silica microspheres produced in the single phase microreactor with an inner diameter of 250  $\mu\text{m}$ .

Residence Time (min)	Single Phase Microreactor (250 $\mu\text{m}$ ID aging capillary)	
5		<p data-bbox="1130 554 1284 583" style="text-align: center;"><i>NO IMAGE</i></p>
10		
15		
20		

### 2.3.3 Segmented Flow Synthesis of Silica

Figures 2.11 and 2.12 show the average microsphere diameters provided by DLS and SEM data for microspheres synthesized in a segmented flow microreactor with a 250  $\mu\text{m}$  ID aging capillary.

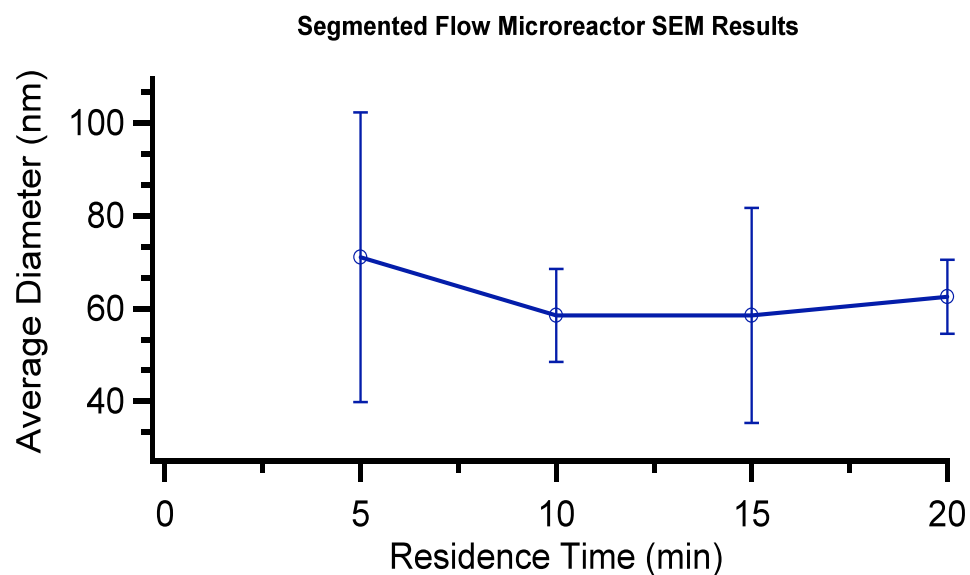


Figure 2.11. Average diameter of silica microspheres produced in the segmented flow microreactor. This data was collected from SEM images.



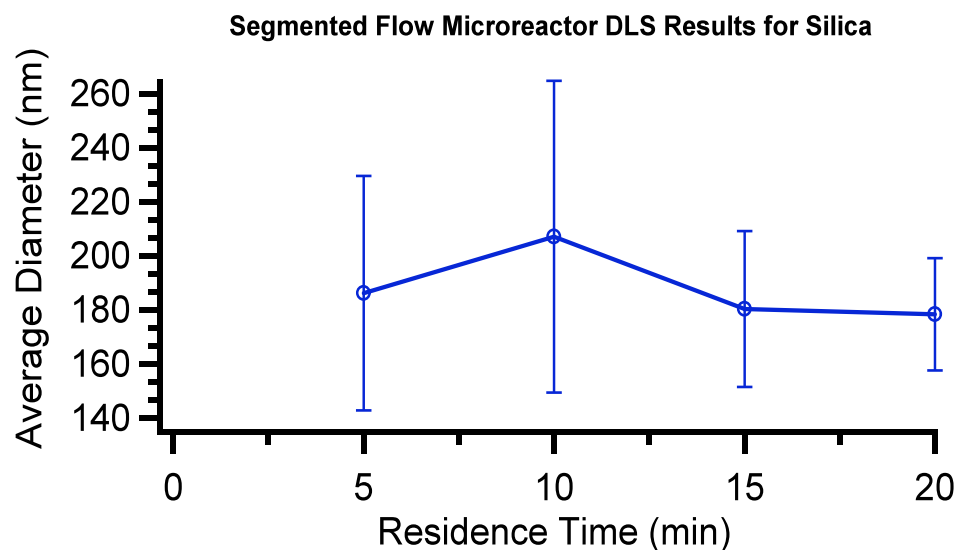
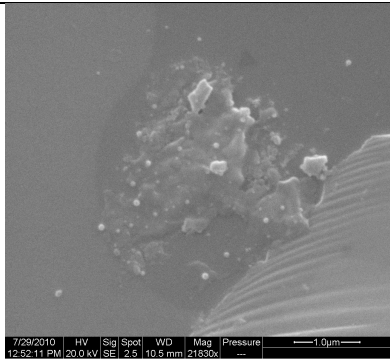
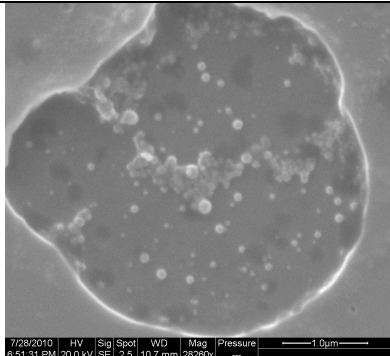
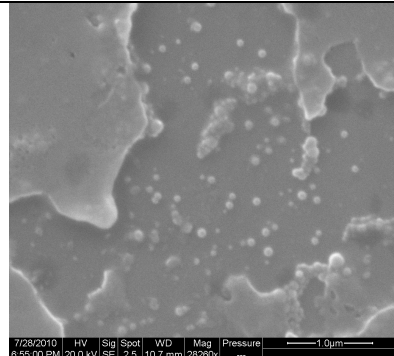
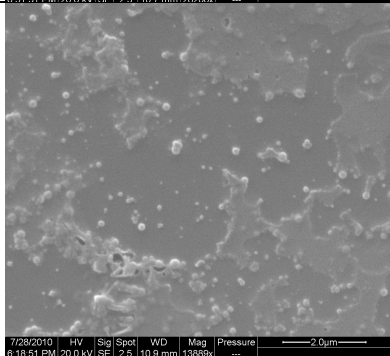
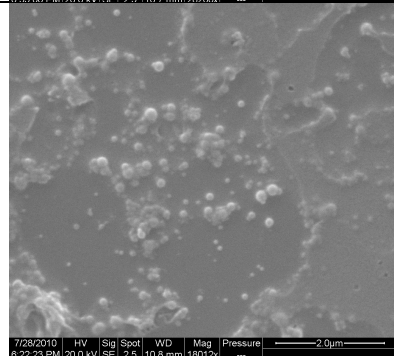
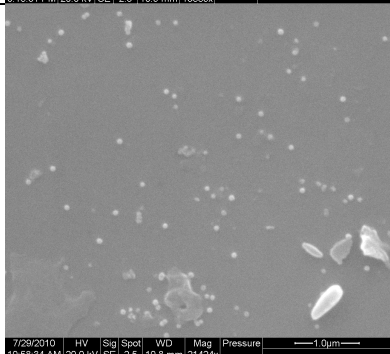
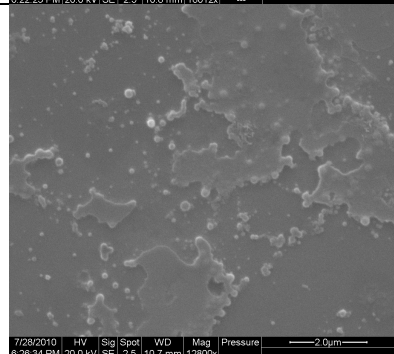


Figure 2.12. Average diameter of silica microspheres produced in the segmented flow microreactor. This data was gathered from DLS

For the 5 minute residence time samples the DLS gives an average diameter of  $186.2 \pm 43.3$  nm ( $n=4$ , 23.2% RSD) while the SEM images give an average diameter of  $71.0 \pm 31.2$  nm ( $n=3$ , 43.9% RSD). The 10 minute residence time samples have an average diameter of  $207.0 \pm 57.6$  nm ( $n=4$ , 27.8% RSD) according to the DLS and  $58.5 \pm 10.0$  nm ( $n=4$ , 17.2% RSD) according to SEM data. For the 15 minute residence time samples the DLS gives an average diameter of  $180.3 \pm 28.8$  nm ( $n=4$ , 16.0% RSD) and the SEM images give an average diameter of  $58.5 \pm 23.2$  nm ( $n=4$ , 39.7% RSD). The 20 minute residence time samples have an average diameter of  $178.3 \pm 20.7$  nm ( $n=4$ , 11.6% RSD) according to the DLS and an average diameter of  $62.5 \pm 8.0$  nm ( $n=4$ , 13% RSD) according to the SEM data. Images of these microspheres are found in Table 2.8.

Table 2.8. SEM images of silica microspheres synthesized in the segmented flow microreactor.

Residence Time (min)	Segmented Flow Microreactor (250 $\mu\text{m}$ ID aging capillary)	
5		<p style="text-align: center;"><i>NO IMAGE</i></p>
10		
15		
20		

The SEM and DLS results both lack evidence of a trend between the residence time and the average diameter, or the standard deviation and % RSD values. Contrary to expectations, the average diameter does not clearly show signs of increasing with longer residence times, nor is the standard deviation less than that of microspheres produced in the batch reactor and the single phase microreactor. The SEM images of these samples in Table 2.8 show that the products do not exhibit a clearly defined spherical morphology which suggests that the reaction did not occur properly within the nano-beakers.

The most likely cause of an improper reaction in the nano-beakers is an incorrect distribution of reagents into the plugs upon segmentation. It is known that the concentration of ammonia and the basic environment that it creates has a significant effect on the size, morphology, and uniform suspension of the product, as discussed earlier.<sup>29, 35, 39</sup> Clearly, an ammonia concentration which is inadequate or which varies from one plug to the next can cause variation in particle size and morphology, including a lack of a distinguished morphology. The concentration of TEOS has also been shown to affect the formation of the particles as well, tending to sabotage the formation of spherical particles when the concentration exceeds 0.5 M. If the original concentrations of the reagents, particularly ammonia and TEOS, were disturbed upon segmentation the nano-beakers would have a random distribution of reagents causing the failure to form distinct microspheres.

The actual distribution of reagents into the slugs occurs in the segmenting T-junction when the gas stream intersects and segments the stream of the two combined reagent solutions. The inner diameter of the aging capillary is 100  $\mu\text{m}$  greater than the inner diameter of the preceding capillaries and the T-junction. This diameter difference was implemented because better results were achieved with a wider aging capillary in the single phase microreactor, and because the back pressure in the system is reduced when the aging capillary is wider than the preceding capillaries and T-junctions. Increasing the inner diameter of the aging capillary even further may improve reagent distribution, although attention must be paid to the capillary number to ensure that wall spanning slugs can still be formed.

When designing the microreactor the intermediate capillary (labeled in Figure 1.19) was intentionally kept short, at about 1 cm in length, to reduce the length over which dispersion and diffusion could occur prior to segmentation. Dispersion needed to be minimized to avoid the widening of the residence time distribution as a result of the parabolic velocity profile. Diffusion needed to be minimized to reduce the amount of mixing that occurred before the reagents entered the aging capillary in order to preserve the accuracy of residence time measurements. The fluid behavior in the intermediate capillary and in the T-junction should be the focus of further investigation into the reagent distribution problem.

### 2.3.4 Batch Synthesis of Titania

Due to the reagent distribution problems involved with the segmented flow microreactor, titania was only synthesized in the batch reactor and the single phase microreactor. The DLS data for all titania samples was disregarded because the polydispersity indices reported by the instrument indicated a very high degree of aggregation that rendered the DLS data inaccurate.

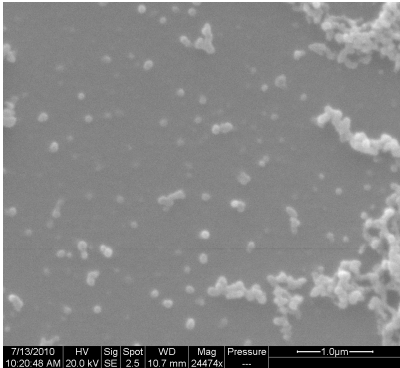
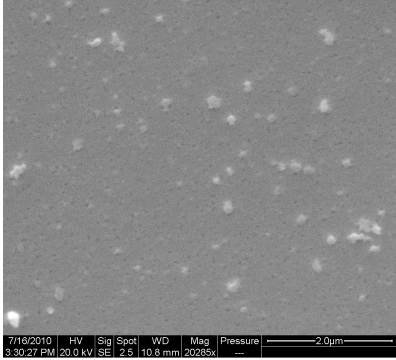
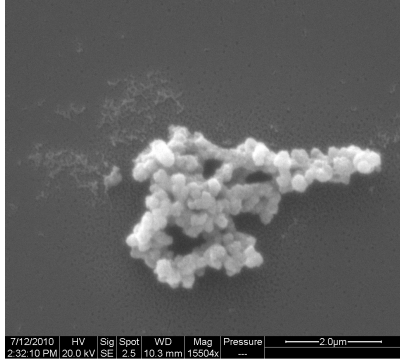
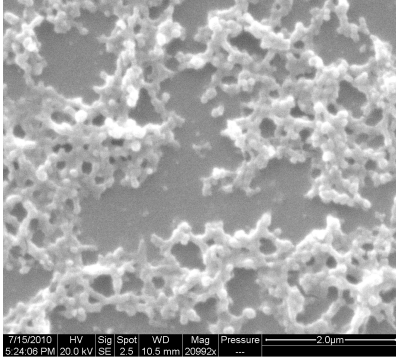
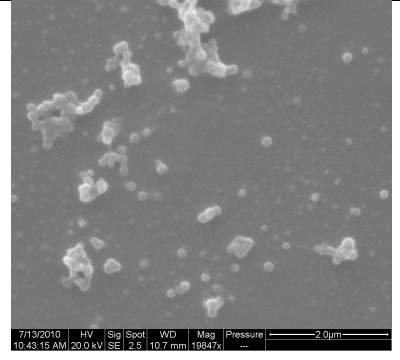
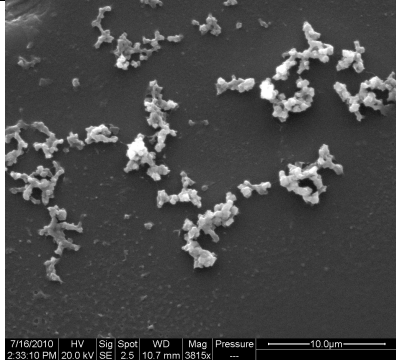
Table 2.9. Microsphere diameter results for the batch synthesis of titania

<b>Mixing Time (min)*</b>	<b>SEM</b>	
	<b>Average Diameter (nm)</b>	<b>Replicates (N)</b>
240	81	1

\*Mixed for 150 minutes, let sit for 90 minutes

The average diameter of microspheres produced by batch synthesis of titania for 240 minutes is 81 nm, as reported in Table 2.9. There were a series of preliminary batch reactions that involved adjustments to the pH, in the form of the concentration of acetic acid, as well as adjustments to R which is the water to titanium isopropoxide ratio. Table 2.10 shows images of the results of these preliminary reactions. The recipe used is indicated by \*\* in Table 2.10 and was considered the best recipe because it produced the most discrete microspheres. This recipe was then used for single phase microreactor synthesis.

Table 2.10. SEM images of titania produced by preliminary batch syntheses for different concentrations of acetic acid and for different water/titanium isopropoxide ratios (R).

Changing $[\text{CH}_3\text{COOH}]$	Changing R
 <p data-bbox="383 865 902 905">**R = 1.7, <math>[\text{CH}_3\text{COOH}] = 6.96 \times 10^{-3} \text{M}</math></p>	 <p data-bbox="984 856 1377 896">R = 1, <math>[\text{CH}_3\text{COOH}] = 0.696 \text{M}</math></p>
 <p data-bbox="422 1304 860 1344">R = 1.7, <math>[\text{CH}_3\text{COOH}] = 0.0696 \text{M}</math></p>	 <p data-bbox="984 1304 1377 1344">R = 3, <math>[\text{CH}_3\text{COOH}] = 0.696 \text{M}</math></p>
 <p data-bbox="431 1751 854 1791">R = 1.7, <math>[\text{CH}_3\text{COOH}] = 0.696 \text{M}</math></p>	 <p data-bbox="984 1751 1377 1791">R = 5, <math>[\text{CH}_3\text{COOH}] = 0.696 \text{M}</math></p>

The rate of mixing in batch synthesis was not regulated and may be part of the cause of some aggregation. Barringer et al observed that higher stirring rates produced more coagulated particles and that the appearance of particle clusters decreased with a decrease in the stirring rate.<sup>40</sup> The pH is not to blame, because the acidic conditions give rise to electrostatic repulsions between particles.<sup>41</sup>

A possible explanation for the poor results is the onset of gelation. Upon further research into the literature, it becomes apparent that the cause of the poorly formed particles is more likely the reagents than the microreactor design, particularly the presence of the acetic acid. Although Hsu et al<sup>41</sup> say that the presence of an acid is necessary to avoid particle aggregation with electrostatic repulsion, many groups report that the presence of an acid is conducive to the formation of gels, not the sols that are needed here.<sup>40, 54</sup> As a result, what at first appeared to be aggregation and poorly formed particles is more accurately considered the beginnings of gelation.

### *2.3.5 Single Phase Microreactor Synthesis of Titania*

The average diameters determined from SEM images for the single phase microreactor synthesis of titania are shown in Figure 2.13. The titania microspheres produced with residence times of 15, 30, and 60 minutes are very similar in average diameter and size distribution and their relationships to one another do not exhibit any clear trends.

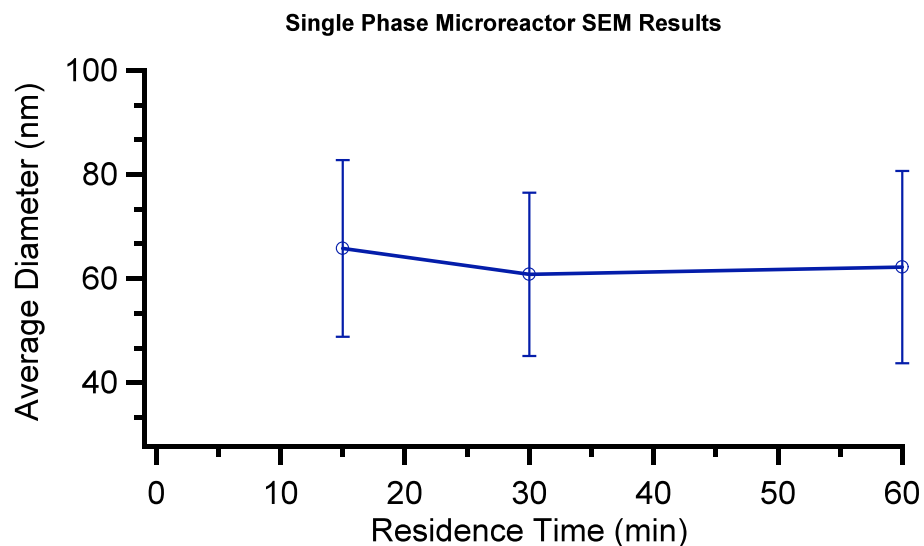
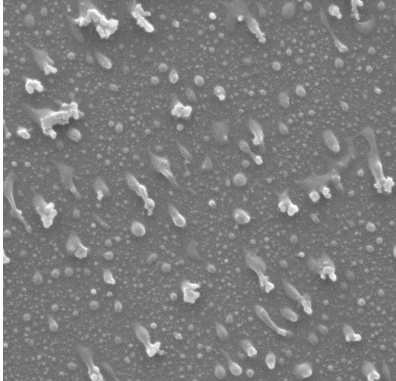
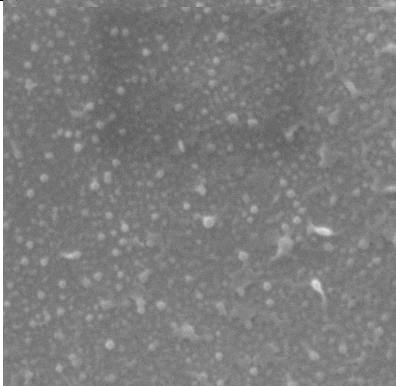
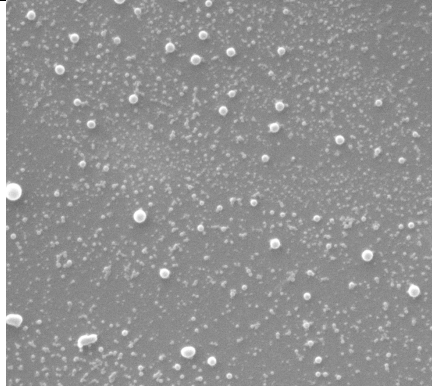
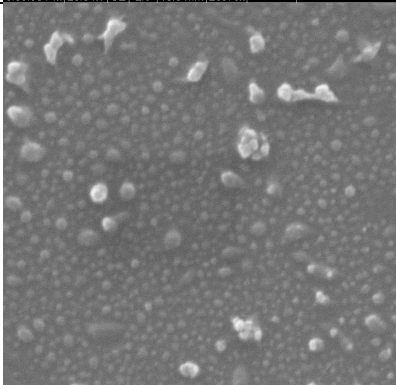
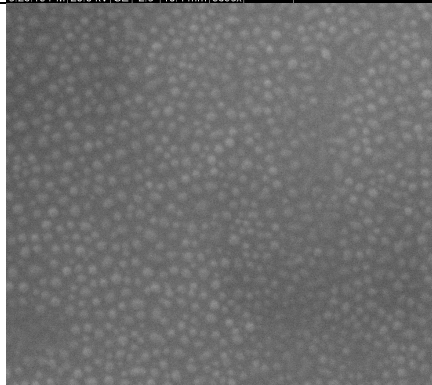


Figure 2.13. Average diameter of titania microspheres produced in the single phase microreactor. This data was collected from SEM images.

The average microsphere diameter is  $65.8 \pm 17.0$  ( $n=5$ , 25.8% RSD),  $60.8 \pm 15.7$  ( $n=5$ , 25.8% RSD), and  $62.2 \pm 18.5$  ( $n=6$ , 29.7% RSD) for 15 minute, 30 minute, and 60 minute residence times, respectively. The average diameter is small for such long residence times compared to those seen for the synthesis of silica. Images of these titania microspheres can be seen in Table 2.11 and show evidence of well formed microspheres.



Table 2.11. SEM images of titania produced in the single phase microreactor

Residence Time (min)	Single Phase Synthesis (250 um ID aging capillary)	
15	 <p>7/22/2010 HV Sig Spot WD Mag Pressure 1:55:45 PM 20.0 kV SE 2.5 10.3 mm 11993x --- 2.0um</p>	NO IMAGE
30	 <p>7/20/2010 HV Sig Spot WD Mag Pressure 6:03:30 PM 20.0 kV SE 2.5 10.8 mm 26375x --- 1.0um</p>	 <p>7/23/2010 HV Sig Spot WD Mag Pressure 3:28:18 PM 20.0 kV SE 2.5 10.4 mm 8893x --- 5.0um</p>
60	 <p>7/23/2010 HV Sig Spot WD Mag Pressure 3:46:42 PM 20.0 kV SE 2.5 10.4 mm 22048x --- 1.0um</p>	 <p>7/20/2010 HV Sig Spot WD Mag Pressure 6:43:35 PM 20.0 kV SE 2.5 10.7 mm 36825x --- 1.0um</p>

The single phase microreactor results produced more clearly formed microspheres than batch synthesis, although they are very polydisperse as is

evident from the SEM images. Images of the batch synthesized titania in Table 2.10 show signs of gelation with the large network-like structures that are present, but these are not seen in the microreactor results. This suggests that the single phase microreactor was able to produce microspheres with a better morphology than the batch reactor, although more experiments need to be carried out for this possibility to be seriously considered.

## CHAPTER 3—CONCLUSIONS

### 3.1 Characterization of Segmented Flow

The results of segmented flow characterization in Chapter 1 show that reproducible multi-phase flows can be achieved in a microreactor constructed with capillary fluidics and, further, that these flows are reproducible. The reproducibility of the flows is confirmed by the consistent periodicity of nano-beaker formation as evidenced by the low standard deviations in average plug volume and rate of formation. The similarity between different trials of these measurements further establishes reproducibility in the segmented flow microreactor.

Since the commercially-based segmented flow microreactor was able to achieve reproducible and periodic segmented flows, it was concluded that this system was suitable for use in the synthesis of ceramic microspheres. Nano-beakers allow for precise control over the reaction time by eliminating the residence time widening effects of dispersion and by isolating the reaction within equally-sized nano-beakers. Reproducible flows of periodic nano-beakers, therefore, have the potential to produce microspheres with narrow size distributions and with diameters that are consistent for a given residence time.

## 3.2 Characterization of Ceramic Microsphere Synthesis

### 3.2.1 *Batch Reactor*

The batch reactor produced silica microspheres after various reaction times with standard deviations between about 2 and 6% RSD, which is indicative of a narrow size distribution. This narrow distribution does not, however, necessarily speak to the reproducibility between separate batches which is required for the large scale production of monodisperse microspheres. The average diameter of silica from separate batches sampled after a twenty minute reaction time range from  $107 \pm 2$  nm to  $211 \pm 36$  nm, but more replicates are needed to make sound conclusions in regards to this issue. The next step in characterizing the batch reactor would be to compare the size distribution between separate batches and for various residence times to confirm the irreproducibility of microsphere synthesis by this method.

The batch reactor produced titania results that were difficult to interpret due primarily to the fact that the pH of the reaction mixture was too acidic, favoring the formation of a gel over a sol of individual particles. The rate of mixing could have contributed to the poor results as well, as Barringer et al observed that higher stirring rates produced more coagulated particles and that the appearance of particle clusters decreased with a decrease in the stirring rate.<sup>40</sup> Refinement of the recipe, mixing rates, and reaction times for titania synthesis is necessary.

### 3.2.2 *Single Phase Microreactor*

The single phase microreactor synthesis of silica was carried out with an aging capillary with an inner diameter of 150  $\mu\text{m}$  as well as 250  $\mu\text{m}$ . The 250  $\mu\text{m}$  aging capillary produced better results in that the microspheres exhibited clearer trends in diameter and size distribution, were more clearly defined, and were found on the SEM for all residence times, which was not the case for the 150  $\mu\text{m}$  samples. Failure to find microspheres with the SEM for the five minute residence time 150  $\mu\text{m}$  samples could be due to the resolution limitations of the microscope since the diameter of these particles would have been less than 100 nm.

The 250  $\mu\text{m}$  aging capillary microreactor produced results that indicated a faster particle growth rate than evidenced in the batch reactor, as these particles achieved an average diameter of 193 nm after a 20 minute residence time when those reacted for 20 minutes in the batch reactor only grew to 107 nm. In both single phase microreactors the microspheres had wider size distributions than the batch reactor, with %RSD values ranging from about 6 to 33% between the two of them. The wide size distributions can be attributed to the effects of axial dispersion in the aging capillary. The extent of dispersion increases with both the faster flow rates characteristic of the shorter residence times and the longer aging capillary lengths that accompany the longer residence times.<sup>23</sup>

The successful synthesis of silica microspheres in the single phase microreactor shows that capillary-based microfluidic devices are a legitimate alternative to microfabricated microreactors for microsphere synthesis.

The titania produced in the single phase microreactor did not exhibit a clear trend in size or size distribution as a result of the acidic reaction conditions discussed previously. The SEM images, however, show signs of clearly formed microspheres that lack the gelation apparent in the batch reactor results. The fact that the single phase microreactor produced microspheres that were better formed and developed than the batch reactor in these trials needs more investigation before it can be seriously considered as a characteristic of the single phase microreactor. Nevertheless, SEM images show that titania microspheres began to form, thereby validating the microreactor as a viable reaction vessel for sol-gel chemistry. Refinement of the recipe for batch titania synthesis is the essential next step so that it can then be transferred to the microreactor and characterized.

### *3.2.3 Segmented Flow Microreactor*

The segmented flow microreactor produced silica microspheres with the widest size distributions for all samples, with %RSD values ranging from 8 to about 32%. This outcome contradicted expectations since the segmentation of the reagent stream into nano-beakers was expected to achieve a narrower size distribution than both the batch reactor and the single phase microreactor. This

was expected because confining the reaction to a series of nano-beakers narrows the residence time distribution by eliminating dispersion. The size distribution was also expected to narrow as a result of the reproducibility and periodicity of slug generation demonstrated in the results from Chapter 1, which should reduce the overall size distribution between several batches.

Because silica microspheres were successfully synthesized in the single phase microreactor and because the SEM images of the segmented flow products show unclear particle morphologies, the problem likely lies in the distribution of reagents into the nano-beakers and does not discount the potential for microsphere synthesis in a capillary-based microreactor. If the concentrations of ammonia within each nano-beaker are too low, or the concentrations of TEOS are too high, the development particles with proper morphology will be impeded.<sup>39</sup> Further, if each nano-beaker has a different mix of reagents the reaction will not proceed as expected and the product will not be uniform or necessarily spherical at all.

The distribution of reagents can be influenced by a variety of factors including the extent of mixing in the intermediate capillary before segmentation, the flow rates of the reagents, and the flow rate of the air, to name a few. The segmented flow microreactor needs further modifications and fine-tuning in order for it to produce monodisperse microspheres. The next step in improving the device would be to investigate the distribution of reagents in the slugs upon

segmentation. There are several ways to go about exploring this problem, none of which are simple tasks.

One possible approach is to replace the two reagent solutions with a transparent liquid and a fluorescent solution. Ideally, the average Peclet number of this system would be close to that of the actual microsphere-producing system so that a similar degree of diffusion would occur in the intermediate capillary before segmentation. An unequal distribution of the two solutions in the nanobeaders would be confirmed after segmentation by a variation in the intensity of the fluorescence of the plugs. These observations can be quantified by obtaining fluorescence spectroscopy measurements of each individual plug. A major difficulty here is the collection of these readings; a customized instrument would have to be assembled with the ability to measure the fluorescence of each of the closely-spaced plugs individually and in a dark environment without any stray light.

### 3.3 Comparison with the literature

The results of this work were compared to data published by Klavs Jensen's research group at the Massachusetts Institute of Technology. Jensen has published papers on a wide range of topics relating to microfluidic devices, including their use for the synthesis of colloidal silica. His group also synthesized silica microspheres in a batch reactor, a single phase microreactor, and a



segmented flow microreactor. Two of the most significant differences between their reaction setup and ours were that their microreactors were microfabricated in PDMS by soft lithography, and their reagent concentrations were twice that of our recipe. The reagents that they used, however, were the same.<sup>5</sup>

This group, like us, found that the batch reactor produced microspheres with a narrower size distribution than the single phase microreactor. Our size distributions were slightly narrower than theirs for both of these cases—their RSD values for the batch reactor ranged from 4 to 9 % for reaction times of five to twenty minutes, while ours ranged from about 2 to 6 % for the same reaction times.

Jensen's group observed the same relationship between the size distributions of microspheres produced by batch synthesis and in a single phase microreactor, in that the microspheres produced in the single phase microreactor had a wider size distribution than those produced by batch synthesis. Their RSD values for the single phase microreactor ranged from about 10 to 22% for residence times of five to twenty minutes, while the microspheres we produced with our commercially-based microreactor had RSD values ranging from about 8 to 25% according to data from SEM images.

Jensen's group achieved the narrowest size distribution with the segmented flow microreactor, with RSD values within the range of about 7 to 11%. Their microfabricated microreactor was able to produce microspheres with

a distinct morphology, whereas ours needs further modification to achieve the same results.

### 3.4 Future Work

This work has shown that a commercially-based microfluidic device is a viable option for producing reproducible and periodic segmented flows, and that ceramic synthesis is possible under single phase flows. It holds promise for the segmented flow synthesis of monodisperse colloidal ceramics, pending modifications to the microreactor to achieve correct distributions of reagents into nano-beakers. Once this is completed, these devices could be used for the production of microspheres with reproducible sizes and narrow size distributions by connecting hundreds or thousands of these devices in parallel. In addition to reproducibility and narrow size distributions, this method of production would be advantageous over traditional batch synthesis methods due to its high yields, low reagent consumption and waste production, and its ease of automation.

REFERENCES

1. Song, Helen, Delai L. Chen, and Rustem F. Ismagilov. "Reactions in Droplets in Microfluidic Channels." *Angewandte Chemie* 45, (2006): 7336-7356.
2. Hartman, Ryan L. and Klavs F. Jensen. "Microchemical Systems for Continuous-Flow Synthesis." *Lab on a Chip* 9, (2009): 2495-2507.
3. Marre, Samuel and Klavs F. Jensen. "Synthesis of Micro and Nanostructures in Microfluidic Systems." *Chemical Society Reviews* 39, (2010): 1183-1202.
4. Trachsel, Franz, Axel Günther, Saif Khan, and Klavs F. Jensen. "Measurement of Residence Time Distribution in Microfluidic Systems." *Chemical Engineering Science* 60, no. 21 (11, 2005): 5729-5737.
5. Khan, Saif A., Axel Günther, Martin A. Schmidt, and Klavs F. Jensen. "Microfluidic Synthesis of Colloidal Silica." *Langmuir* 20, (2004): 8604-8611.
6. Atencia, Javier and David J. Beebe. "Controlled Microfluidic Interfaces." *Nature* 437, (2005): 648-655.
7. Fiorini, Gina S. and Daniel T. Chiu. "Disposable Microfluidic Devices: Fabrication, Function, and Application." *BioTechniques* 38, (2005): 429-446.
8. Li, Liang, James Q. Boedicker, and Rustem F. Ismagilov. "Using a Multijunction Microfluidic Device to Inject Substrate into an Array of Preformed Plugs without Cross-Contamination: Comparing Theory and Experiments." *Analytical Chemistry* 79, no. 7 (04/01, 2007): 2756-2761.
9. Stelick, Scott J., William H. Alger, Jesse S. Laufer, Anna M. Waldron, and Carl A. Batt. "Hands-on Classroom Photolithography Laboratory Module to Explore Nanotechnology." *Journal of Chemical Education* 82, no. 9 (09/01, 2005): 1361-null.
10. Günther, Axel, Manish Jhunjhunwala, Martina Thalmann, Martin A. Schmidt, and Klavs F. Jensen. "Micromixing of Miscible Liquids in Segmented Gas-Liquid Flow." *Langmuir* 21, no. 4 (02/01, 2005): 1547-1555.

11. Günther, Axel and Klavs F. Jensen. "Multiphase Microfluidics: From Flow Characteristics to Chemical and Materials Synthesis." *Lab on a Chip* 6, (2006): 1487-1503.
12. Laval, Philippe, Nicolas Lisai, Jean-Baptiste Salmon, and Mathieu Joanicot. "A Microfluidic Device Based on Droplet Storage for Screening Solubility Diagrams." *Lab on a Chip* 7, (2007): 829-834.
13. Lorenz, Robert M., J. S. Edgar, Gavin D. M. Jeffries, and Daniel T. Chiu. "Microfluidic and Optical Systems for the on-Demand Generation and Manipulation of Single Femtoliter-Volume Aqueous Droplets." *Analytical Chemistry* 78, no. 18 (09/01, 2006): 6433-6439.
14. Wu, Hongkai, Teri W. Odom, Daniel T. Chiu, and George M. Whitesides. "Fabrication of Complex Three-Dimensional Microchannel Systems in PDMS." *Journal of the American Chemical Society* 125, no. 2 (01/01, 2003): 554-559.
15. Linder, Vincent, Samuel K. Sia, and George M. Whitesides. "Reagent-Loaded Cartridges for Valveless and Automated Fluid Delivery in Microfluidic Devices." *Analytical Chemistry* 77, no. 1 (01/01, 2005): 64-71.
16. Garstecki, Piotr, Michael J. Fuerstman, Howard A. Stone, and George M. Whitesides. "Formation of Droplets and Bubbles in a Microfluidic T-junction—scaling and Mechanism of Break-Up." *Lab on a Chip* 6, (2006): 437-446.
17. Spriggs, H. D. "Comments on Transition from Laminar to Turbulent Flow." *Industrial & Engineering Chemistry Fundamentals* 12, no. 3 (08/01, 1973): 286-290.
19. Taylor, Geoffrey. "Dispersion of Soluble Matter in Solvent Flowing Slowly through a Tube." *Proceedings of the Royal Society of London. Series A. Mathematical and Physical Sciences* 219, (1953): 186-203.
20. Tian, Wei-Chang and Erin Finehout. *Microfluidics for Biological Applications* Springer US, 2009.
21. "Bright Field Versus Dark Field." <http://www.darkfield-microscope.com/bright-field-versus-dark-field.html>(2010).

22. Stone, H. A., A. D. Stroock, and A. Ajdari. "Engineering Flows in Small Devices: Microfluidics Toward a Lab-on-a-Chip." *Annual Review of Fluid Mechanics* 36, (2004): 381-411.
23. Squires, Todd M. and Stephen R. Quake. "Microfluidics: Fluid Physics at the Nanoliter Scale." *Reviews of Modern Physics* 77, (2005): 977-1026.
24. Griffin, Steve. Fused-Silica Capillary--the Story Behind the Technology. *LC-GC Europe*, 2003. 1.
25. "Fluid Mechanics: Overview." efunda.  
<http://www.efunda.com/formulae/fluids/overview.cfm> (2011).
26. Duffy, David C., J. Cooper McDonald, Olivier J. A. Schueller, and George M. Whitesides. "Rapid Prototyping of Microfluidic Systems in Poly(Dimethylsiloxane)." *Analytical Chemistry* 70, (1998): 4974-4984.
27. Kim, Pilnam, Keon Woo Kwon, Min Cheol Park, Sung Hoon Lee, Sun Min Kim, and Kahp Yang Suh. "Soft Lithography for Microfluidics: A Review." *BioChip Journal* 2, (2008): 1-11.
28. McDonald, J. Cooper and George M. Whitesides.  
"Poly(Dimethylsiloxane) as a Material for Fabricating Microfluidic Devices." *Accounts of Chemical Research* 35, no. 7 (2002): 491-499.
29. Brinker, C. Jeffrey and George W. Scherer. *Sol-Gel Science: The Physics and Chemistry of Sol-Gel Processing*. San Diego: Academic Press, Inc, 1990.
30. *Handbook of Sol-Gel Science and Technology: Processing, Characterization, and Applications*, edited by Sumio Sakka. Vol. 1. New York: Kluwer Academic Publishers, 2005.
31. Pierre, Alain C. *Introduction to Sol-Gel Processing*. Norwell, MA: Kluwer Academic Publishers, 1998.
32. Brown, Theodore L., H. Eugene LeMay, and Bruce E. Bursten.  
*Chemistry: The Central Science*, edited by Nicole Folchetti, John Challice. 10th ed. Upper Saddle River, NJ: Pearson Education Inc, 2006.
33. Chen, Yongjun and Dionysios D. Dionysiou. "Sol-Gel Synthesis of Nanostructured TiO<sub>2</sub> films for Water Purification." In *Sol-Gel Methods for Materials Processing*, edited by Plinio Innocenzi, Yuriy L. Zub and Vadim G. Kessler, 67-75: Springer Netherlands, 2008.

34. Gaishun, Vladimir E., Yanina A. Kosenok, Dmitry L. Kovalenko, and Alina V. Semchenko. "Sol-Gel Process Preparation of Functional Silica Materials and their Application." In *Sol-Gel Methods for Materials Processing*, edited by Plinio Innocenzi, Yuriy L. Zub and Vadim G. Kessler, 297-305: Springer Netherlands, 2008.
35. Hench, Larry L. and Jon K. West. "The Sol-Gel Process." *Chemical Reviews* 90, (1990): 33-72.
36. Kessler, Vadim G., Gerald I. Spijksma, Gulaim A. Seisenbaeva, Sebastian Hakansson, Dave H. A. Blank, and Henny J. M. Bouwmeester. "New Insight in the Role of Modifying Ligands in the Sol-Gel Processing of Metal Alkoxide Precursors: A Possibility to Approach New Classes of Materials." *Journal of Sol-Gel Science and Technology* 40, (2006): 163-179.
37. Schottner, Gerhard. "Hybrid Sol-Gel-Derived Polymers: Applications of Multifunctional Materials." *Chemistry of Materials* 13, (2001): 3422-3435.
39. Stober, Werner and Arthur Fink. "Controlled Growth of Monodisperse Silica Spheres in the Micron Size Range." *Journal of Colloid and Interface Science* 26, (1968): 62-69.
40. Barringer, Eric A. and H. Kent Bowen. "High-Purity, Monodisperse TiO<sub>2</sub> Powders by Hydrolysis of Titanium Tetraethoxide. 1. Synthesis and Physical Properties." *Langmuir* 1, (1985): 414-420.
41. Hsu, Jyh-Ping and Anca Nacu. "On the Factors Influencing the Preparation of Nanosized Titania Sols." *Langmuir* 19, (2003): 4448-4454.
42. Madou, Marc J. "Lithography." Chap. 1, In *Fundamentals of Microfabrication*. 2nd ed., 1-76. Boca Raton: CRC Press, 2002.
43. Nguyen, Nam-Trung and Steven T. Wereley. *Fundamentals and Applications of Microfluidics*. Norwood, MA: Artech House, Inc, 2002.
44. "Caltech's Curious Character: Richard Feynman."  
[http://today.caltech.edu/today/story-display.tcl?story\\_id=293](http://today.caltech.edu/today/story-display.tcl?story_id=293).
45. Feynman, Richard P. There's Plenty of Room at the Bottom. *Engineering and Science*, 1960.

46. McMullen, Jonathan P. and Klavs F. Jensen. "Integrated Microreactors for Reaction Automation: New Approaches to Reaction Development." *Annual Review of Analytical Chemistry* 3, (2010): 19-42.
47. Binns, Chris. "The Nanotechnology Toolkit." Chap. 4, In *Introduction to Nanoscience and Technology*, 96-132. Hoboken, NJ: John Wiley & Sons, Inc, 2010.
48. Madou, Marc J. "Lithography." Chap. 1, In *Fundamentals of Microfabrication: The Science of Miniaturization*. 2nd ed., 1-41: CRC Press, 2002.
49. "Flexible Fused Silica Capillary Tubing." Polymicro Technologies.  
[http://www.polymicro.com/products/capillarytubing/products\\_capillarytubing\\_tsp\\_tsg.htm](http://www.polymicro.com/products/capillarytubing/products_capillarytubing_tsp_tsg.htm).
50. "Tools for Science and Medicine." Valco Instruments Co. Inc.  
<http://www.vici.com/>.
51. Erickson, David and Dongqing Li. "Integrated Microfluidic Devices." *Analytica Chimica Acta* 507, (2004): 11-26.
52. "Thermoelectric/ Peltier Cooling." Watronix, Inc.  
<http://www.inbthermoelectric.com/peltier-cooling-and-seebeck-effect.html>.
53. Robello, Doug. "Quantum Amplification: The Key to Speed." Kodak.  
<http://pluggedin.kodak.com/pluggedin/post/?id=655003>.
54. Khalil, Kamal M. S., Thomas Baird, Mohamed I. Zaki, Ahmed A. El-Samahy, and Aida M. Awad. "Synthesis and Characterization of Catalytic Titanias Via Hydrolysis of Titanium (IV) Isopropoxide." *Colloids and Surfaces A* 132, (1998): 21-44.
55. "Dynamic Light Scattering." Malvern.  
[http://www.malvern.com/LabEng/technology/dynamic\\_light\\_scattering/dynamic\\_light\\_scattering.htm](http://www.malvern.com/LabEng/technology/dynamic_light_scattering/dynamic_light_scattering.htm).